Homocoupling Reactions of Azoles and Their Applications in Coordination Chemistry

Steffen B. Mogensen [1], Mercedes K. Taylor [2],* and Ji-Woong Lee [1],*

[1]   Department of Chemistry, University of Copenhagen, Universitetsparken 5, 2100 Copenhagen Ø, Denmark;
     lng656@alumni.ku.dk
[2]   Center for Integrated Nanotechnologies, Sandia National Laboratories, Albuquerque, NM 87185, USA
*   Correspondence: mercedes.taylor@sandia.gov (M.K.T.); jiwoong.lee@chem.ku.dk (J.-W.L.);
     Tel.: +45-35333312 (J.-W.L.)

Abstract: Pyrazole, a member of the structural class of azoles, exhibits molecular properties of interest in pharmaceuticals and materials chemistry, owing to the two adjacent nitrogen atoms in the five-membered ring system. The weakly basic nitrogen atoms of deprotonated pyrazoles have been applied in coordination chemistry, particularly to access coordination polymers and metal-organic frameworks, and homocoupling reactions can in principle provide facile access to bipyrazole ligands. In this context, we summarize recent advances in homocoupling reactions of pyrazoles and other types of azoles (imidazoles, triazoles and tetrazoles) to highlight the utility of homocoupling reactions in synthesizing symmetric bi-heteroaryl systems compared with traditional synthesis. Metal-free reactions and transition-metal catalyzed homocoupling reactions are discussed with reaction mechanisms in detail.
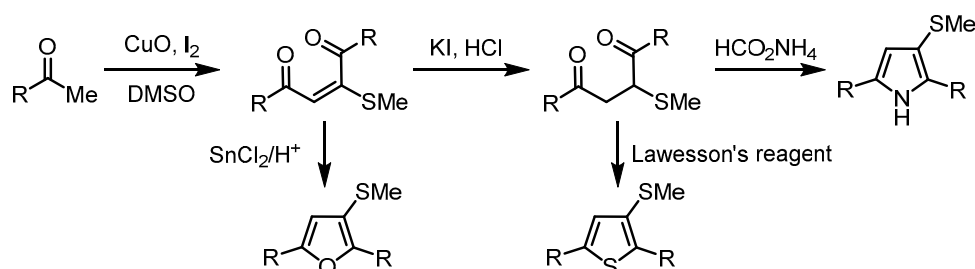
1. Introduction

Heterocyclic compounds containing two or more nitrogen atoms display unique molecular properties, which can be extended to macroscale properties in materials chemistry [1]. Furthermore, symmetric, multiply-functionalized organic ligands are required to construct ordered materials, preferably in high crystallinity [2]. Homocoupling reactions of aromatic compounds are often utilized to form carbon–carbon bonds in the presence of (over)stoichiometric or catalytic amounts of transition metal species [3]. For example, Ullmann coupling reactions can enable facile access to symmetric biaryl compounds using copper reagents with or without ligands at high reaction temperatures [4,5]. Based on this method, a plethora of reports was dedicated to the homocoupling of aromatic compounds, accessing symmetric molecules starting from simple aryl halides and derivatives. However, the reported procedures are often limited in terms of substrate scopes, particularly with heterocyclic compounds. Therefore, milder and more practical reaction conditions are required. To this end, this review summarizes recent development in (catalytic)homocoupling reactions of 5-membererd ring heterocycles, particularly focusing on pyrazoles due to their importance in materials chemistry as symmetric bipyrazoles. First, we will discuss traditional syntheses of bipyrazoles without homocoupling reaction methods, to highlight the advantages of (catalytic)homocoupling reactions. The following sub-chapters are organized by metal-catalyzed and metal-free reactions to illustrate the developed synthetic methods. The utility of bipyrazole materials in materials chemistry is discussed in Section 3.3, where we provide ample information on constructing metal–organic frameworks based on bipyrazole ligands.
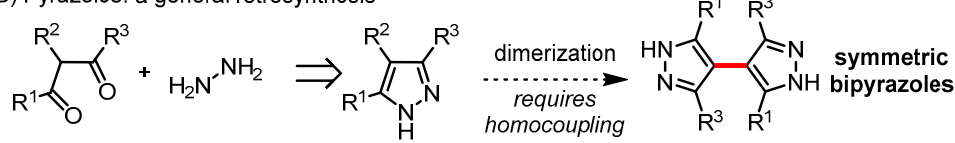
2. Traditional Syntheses of Bipyrazoles

Condensation reactions of 1,4-dicarbonyl compounds with heteroatom nucleophiles can provide various 5-membered heterocycles: furans, thiophenes, pyrroles and their derivatives (Scheme 1A) [6,7]. To access pyrazoles with the same manner, 1,3-dicarbonyl compounds and hydrazine are required (Scheme 1B). However, the lack of a general method of "dimerization" of pyrazole substrates was a major bottleneck for the synthesis of symmetric bipyrazoles. Alternatively, diamino substrates can be prepared to access pyrazoles via oxidation reactions [8]. In 1964, Trofimenko reported the synthesis of 1,1,2,2-ethanetetracarbaldeyde, which was converted to bipyrazole by a condensation reaction with hydrazine (Scheme 1C) [9]. There are a few synthesis methods to access bipyrazoles via lengthy synthetic steps starting from diethyl succinate via a 3,4-carbonyl furan intermediate (**1**) [9–11].
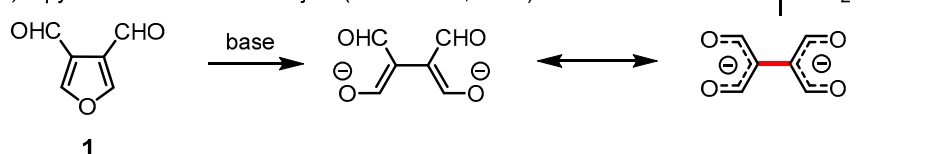

Scheme 1. A comparison of syntheses of 5-membered heterocyclic compounds and pyrazoles.

Starting from succinic ester, a repeated formylation and acetal protection sequence afforded the 3,4-dicarboxylic furan intermediate **2** after treating with concentrated sulfuric acid in 66–68% yield (Scheme 2A). The reaction employed sodium metal and orthoformate for formylation reactions. The author reported that the reaction was amenable to characterize bipyrazole via acetylation, carbamoylation, bromination, dihydrochloride and dinitrate salt. The preparation of 3,4-dicarbonylated furan was further subjected to formylation reactions, and subsequent condensation reactions with hydrazine afforded bipyrazole. For example, the synthesis of furan, thiophene and pyrrole-3,4-dicarboxylic esters was reported, which can allow one to access an intermediate **3** for bipyrazole synthesis [10].
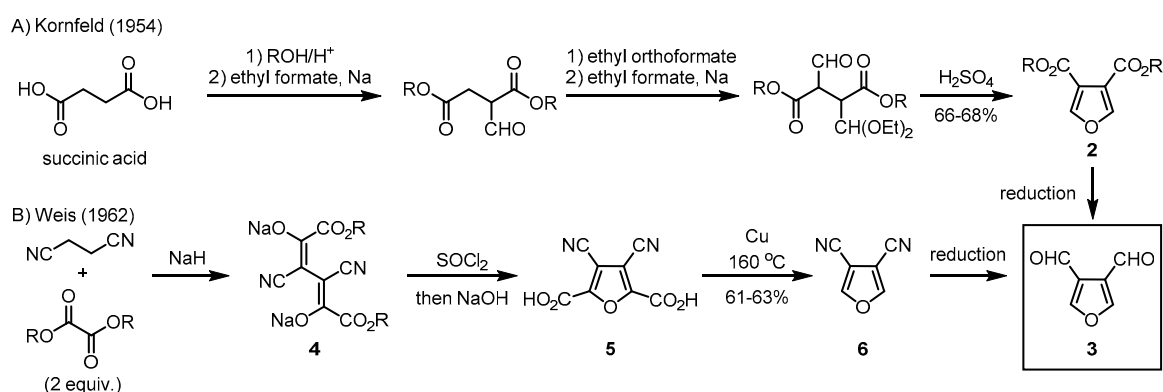
Scheme 2. Syntheses of 3,4-dicarbaldehyde furan **3**.

This procedure started with butyronitril undergoing a Claisen condensation reaction to afford sodium or potassium enolates **4**, which were then treated with SOCl$_2$ to afford 3,4-dicyano-2,5-furandicarboxylate **5**. This compound was further subjected to decarboxylation reaction conditions with copper powder and heated to 160 °C, yielding 61–63% of the product (**6**) [12]. Using this dicyanofuran (**6**), Weis pursued reduction using DIBAL-H to access the dialdehyde compound (**3**). The author found that the compound is stable under acidic conditions; however, it was converted to the ring-opened form under basic conditions, resulting in the formation of the anionic form of tetraaldehyde. This procedure represents a classic synthesis of bipyrazole using a condensation reaction, but Domasevitch and co-workers reported that the procedure was not amenable for the synthesis of bipyrazole [13]. The alternative synthetic approach was started from a dialdehyde, acetylene and formaldehyde to generate an intermediate bis-trimethinium salt (Figure 1) [14]. The synthesis consists of a similar approach as the above-mentioned pathway: a formylation reaction to access tetraaldehyde compounds, which are masked as enamine and iminium functionalities. This sequence requires the use of phosgene and additional steps to finally synthesize bipyrazole.
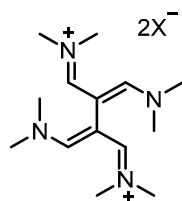

Figure 1. bis-trimethinium salt.

Despite the high application potential of symmetric nitrogen-containing compounds in materials chemistry and coordination chemistry as tunable ligands, the synthetic procedures have been limited to traditional condensation reactions with low atom economy and redox efficiency. Not only are double condensation reactions difficult to control, but the lack of 1,3-dicarbonyl compounds has also hampered the development of facile preparation of pyrazole-based compounds. Therefore, many catalytic systems based on transition-metal catalysts have been investigated owing to the development of cross-coupling reactions, which will be discussed in this review.

3. Recent Advancement of Bipyrazole Syntheses

### 3.1. Transition Metal-Catalyzed Homocoupling of Azoles

Transition metal catalysts play an important role in the functionalization of C–H bonds of aromatic compounds and heteroaromatics and in the formation of new C–C bonds in the synthesis of homocoupled biaryl compounds [3]. The development in homocoupling reactions of pyrazoles, imidazoles and triazoles showed a broad range of catalytic activities in transition metals, including Cu,

Fe, Ni, Pd, Rh and Ru, which were summarized in a review in 2012 [15]. This review will therefore summarize more recent examples (2010–2020) of homocoupling reactions of pyrazoles and azoles (imidazoles, triazoles, tetrazoles) and related compounds.
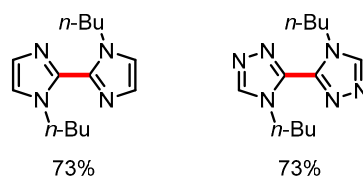
3.1.1. Cu-Catalyzed Homocoupling of Various Azoles

The (oxidative) Glaser–Hay coupling reaction utilizes Cu(I) species as catalysts in the presence of a base under air to afford homo-coupled alkyne products [16]. An adaptation of the Glaser–Hay coupling reaction conditions to *N*-substituted 1,2,4-triazoles was realized starting from easily accessible triazole compounds. In 2009, Do and Daugulis developed Cu(II)-catalyzed homocoupling reactions of imidazoles using molecular oxygen as a terminal oxidant (Scheme 3) [17]. The method developed proved useful in the coupling of various heterocycles, including examples of a *N*-butyl-substituted imidazole and triazole, providing the desired products in up to 73% yield. The mechanism of the reaction was suggested to proceed via deprotonation of heteroarenes (pK$_a$ < 35–37 for C2-H), followed by the complexation with metal additives, such as Li$^+$. The *trans*-metalation step with the copper catalyst and subsequent oxidation yields the intermolecular homocoupling products between two arenes (Scheme 3).
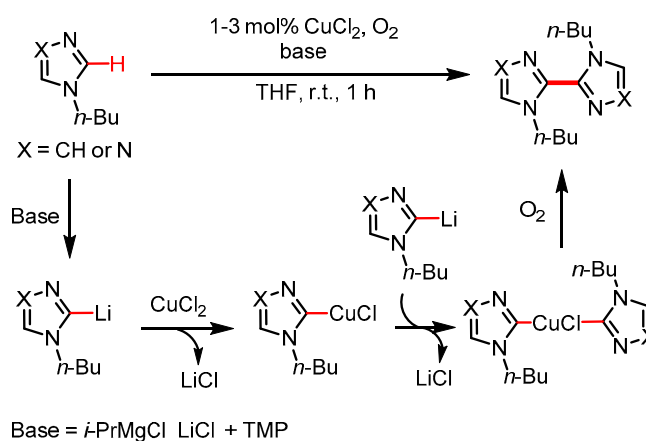

Scheme 3. (**a**) Glaser–Hay type copper catalyzed homocoupling of various azoles resulting in homocoupling using molecular oxygen as a terminal oxidant. (**b**) Substrate scope for the copper catalyzed homocoupling.

Li et al. reported Cu(II)-mediated homocoupling reactions using a similar system at elevated temperatures (Scheme 4) [18]. This method utilizes an efficient and convenient approach to form C2-C2 bonds via a Cu(OAc)$_2$ and O$_2$-mediated oxidative intermolecular homocoupling reaction between two azoles. Once again, the oxidative coupling could be used to achieve high yields of homocoupled products.

a) Reaction conditions
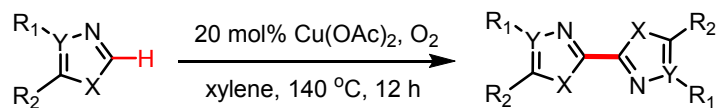
X = N-Me, N-Ph, N-Bn, O
Y = C, N
R = H, Ph, Me

b) Suggested mechanism

c) Substrate scope

90%

91%

80%

83%

81%

75%
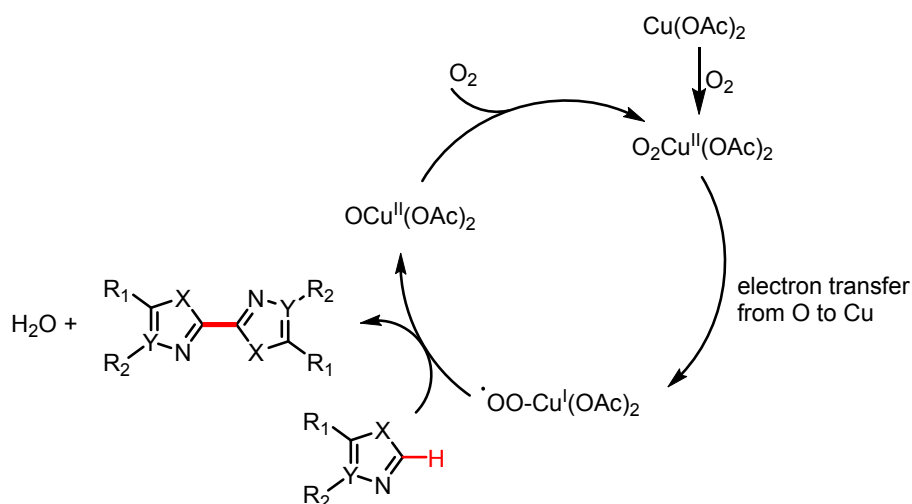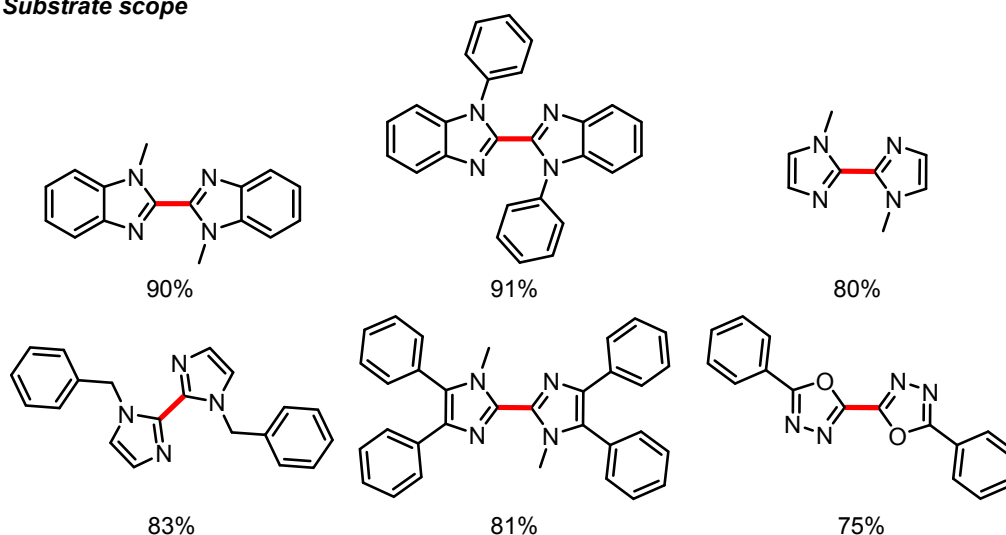
Scheme 4. Copper catalyzed homocoupling of various imidazoles using Cu[II] as the catalyst and molecular oxygen. (**a**) Reaction conditions. (**b**) Suggested mechanism for the homocoupling reaction. (**c**) Substrate scope.

3.1.2. Pd-Catalyzed Homocoupling Reactions of Pyrazoles and Triazoles

Pd-catalyzed cross-coupling reactions are currently classified as some of the most flexible and valuable tools in organic synthesis [19,20]. A common observation is that Pd-catalyzed coupling reactions provide low but significant amounts of homocoupled by-products during cross-coupling reactions [21]. This is likely because the main focus of Pd-catalyzed coupling reactions is to form

bonds between two different coupling partners, enabling highly productive homocoupling reactions. A handful of papers [22,23] have used the tactical placement of heteroatoms for the coordination of metals in the activation of specific C–H bonds. Other papers [24,25] utilize the possibility of the oxidative addition of Pd into a carbon halogen bond to form di-azole Pd complexes, which can undergo reductive elimination to form desired intermolecular homocoupled products.

In 2012, the unexpected discovery of the intermolecular homocoupling between two pyrazoles was made by Salanouve et al. (Scheme 5) [22]. In an effort to study the reaction products obtained under different Suzuki–Miyaura conditions, this group discovered the formation of a C3–C3 intermolecular homocoupled product, resulting from C–H activation. The discovered bipyrazole compound was found to originate from a bis(3-ethoxy-1-(pyridin-2-yl)-1H-pyrazol-5-yl) palladium complex. Through oxidation with NCS, this species forms a Pd^IV complex, which then allows for reductive elimination of the homocoupled product in a yield of up to 34 % (Scheme 5b).
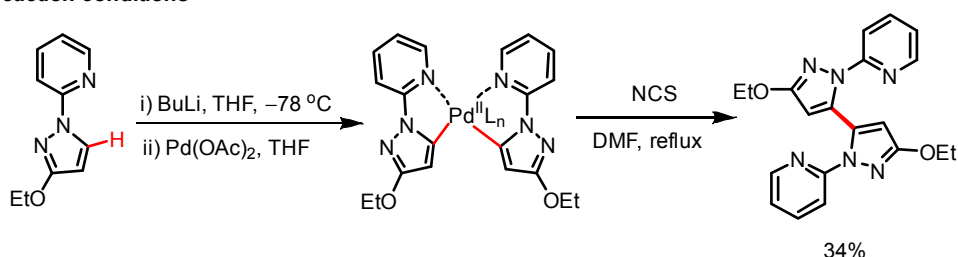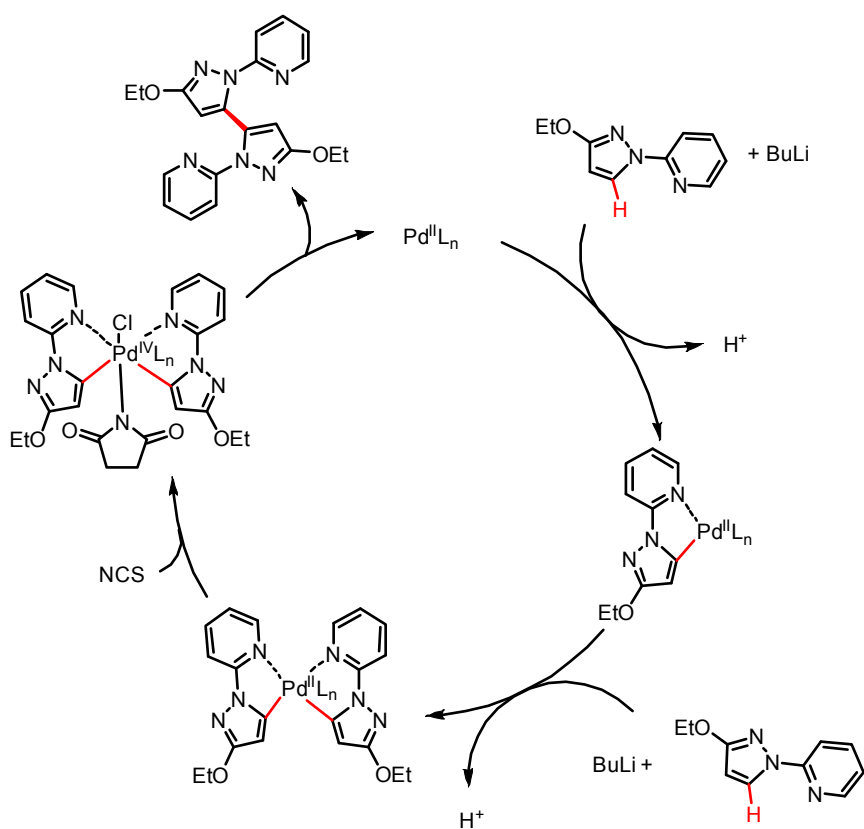
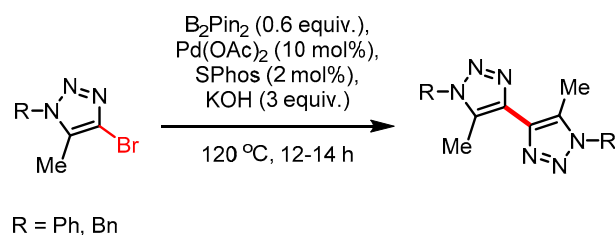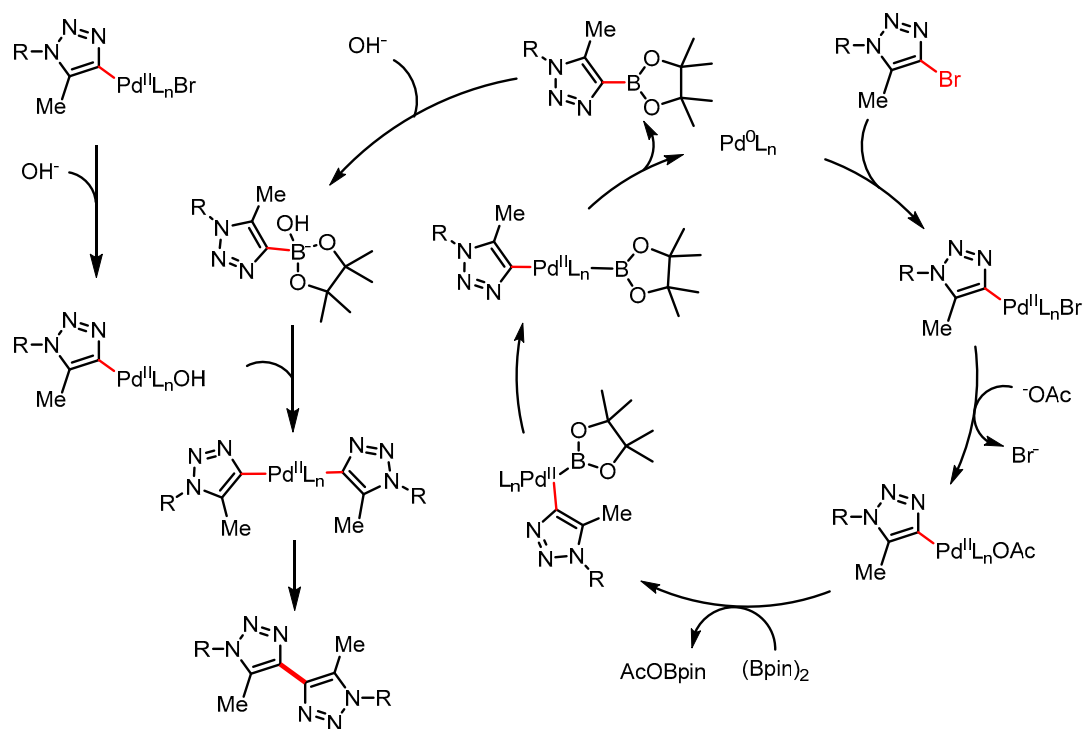**Scheme 5.** (**a**) Reaction conditions for the homocoupling of pyrazoles through formation of a bis(3-ethoxy-1-(pyridin-2- yl)-1H-pyrazol-5-yl) palladium complex followed by oxidation by NCS. (**b**) Suggested mechanism for the C–H activation followed by homocoupling.

Afanas'ev et al. reported a method for the homocoupling of 4-bromo-1,2,3-triazoles to access the corresponding 4,4′-bistriazoles in quantitative yields [24]. The intermolecular homocoupling was achieved by mixing 4-brominated triazoles with 1.0 mol% Pd(OAc)$_2$, in the presence of additives (pinB)$_2$, SPhos and KOH. This method is practical due to the use of readily available starting compounds and a simple experimental procedure, without inert atmosphere or solvent. The reaction possibly occurs through the formation of a 4-Bpin-substituted 1,2,3-triazole. Then, in a Suzuki–Miyaura fashion, the homocoupling of the boronic acid can occur (Scheme 6b).
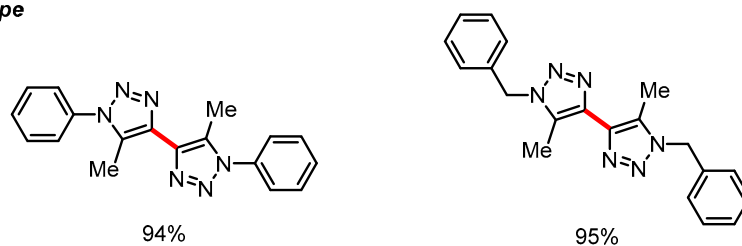
a) Reaction conditions

b) Suggested mechanism

c) Substrate scope

94%

95%

**Scheme 6.** (**a**) Conditions for the homocoupling of 4-bromo-1,2,3-triazoles using Suzuki–Miyaura reaction conditions (**b**) Our suggested mechanism for the homocoupling. (**c**) Substrate scope for the Suzuki–Miyaura homocoupling reaction.

A palladium-catalyzed, pyrazole-directed C(sp^2)−H functionalization of the *N*-phenyl ring in *N*-phenylpyrazoles to afford a biaryl bis-pyrazole (via dehydrogenative homocoupling) was reported by Batchu et al. [23]. Multiple factors were shown to have significant influences on the outcome of the reaction. For example, it was discovered that if the reaction was performed under ca. 10 times dilution, then no homocoupling product was observed, and *N*-(*o*-hydroxyphenyl)pyrazoles were the major or the sole products. The reaction mechanism is suggested in Scheme 7b. After the first C–H activation, the Pd^{II}-center is oxidized to Pd^{IV}, which undergoes a second C–H activation followed by a reductive elimination to yield the homocoupled bipyrazole.

a) Reaction conditions
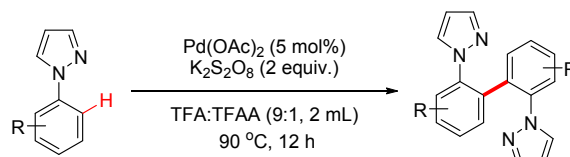
b) Suggested mechanism
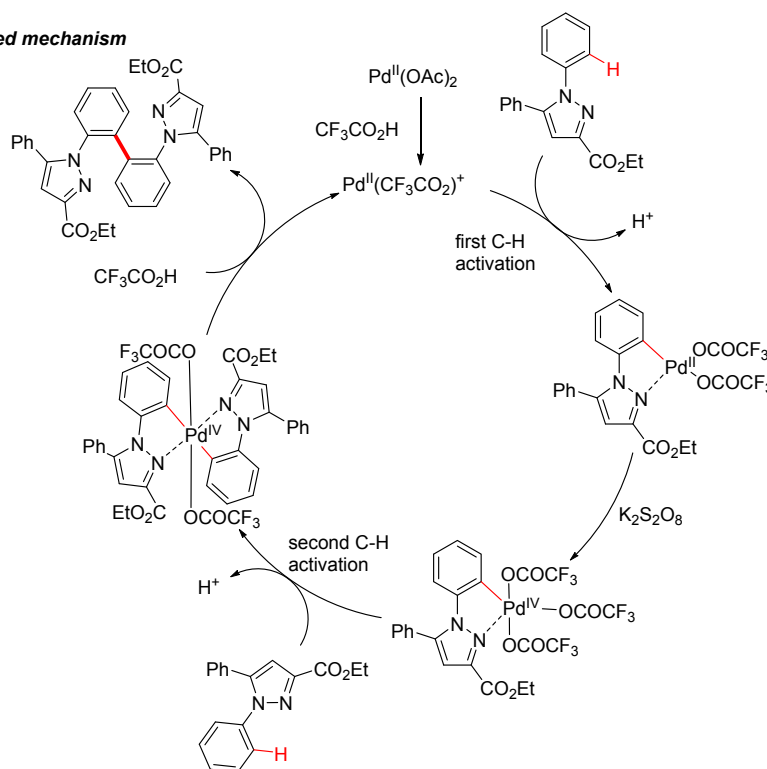
c) Substrate scope
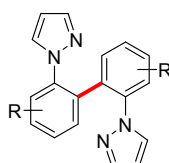
R = H (68%), 2-Cl (83%), 2-Me (80%), 2-CF$_3$ (74%), 2-CO$_2$Et (60%),
3-F (45%), 3-Cl (48%), 4-F (78%), 4-Cl (75%), 4-Br (70%),
4-Me (72%), 4-CF$_3$ (74%), 4-CO$_2$Et (72%), 2,4-Me$_2$ (74%), 3,4-Me$_2$ (70%)

Scheme 7. (**a**) Homocoupling of *N*-phenylpyrazoles through Pd^{II} catalyzed C–H activation of phenyl protons. (**b**) The mechanism for the homocoupling is suggested to go through C–H activation on the phenyl ring followed by formation of a Pd^{IV} specie and then subsequent C–H activation which allows for the reductive elimination of the homocoupled product (**c**) Substrate scope for the homocoupling of various *N*-phenylpyrazole.

The homocoupling reaction between 1,2,3-triazole *N*-oxides by C–H activation at the C4 position was explored by Zhu et al. (Scheme 8) [26]. The reaction was designed to couple 1,2,3-triazole *N*-oxides with sodium arenesulfinates via palladium-catalyzed desulfitative cross-coupling, but it showed the possibility of homocoupling between 1,2,3-triazole *N*-oxides. Under unoptimized reaction conditions, the homocoupled *N*-oxide bistriazoles were generated with yields of up to 22%. The reaction likely occurs via deprotonation followed by exchange of OAc$^-$ for the deprotonated 1,2,3-triazole *N*-oxides. The di-triazole *N*-oxide Pd^{II} complex then undergoes reductive elimination to yield the homocoupled bistriazole *N*-oxide product and Pd^0, which can be oxidized by Ag$_2$CO$_3$.

a) Reaction conditions
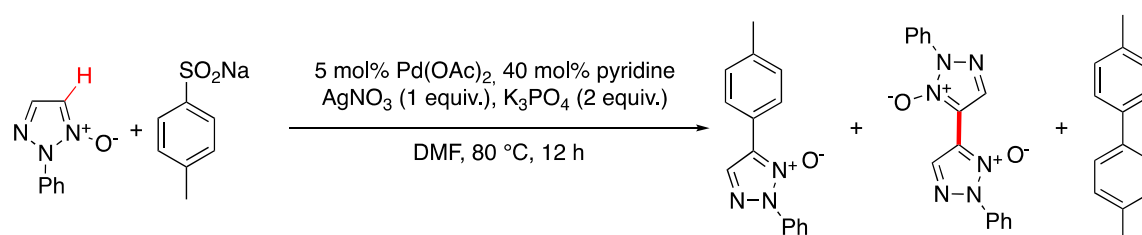
b) Suggested mechanism
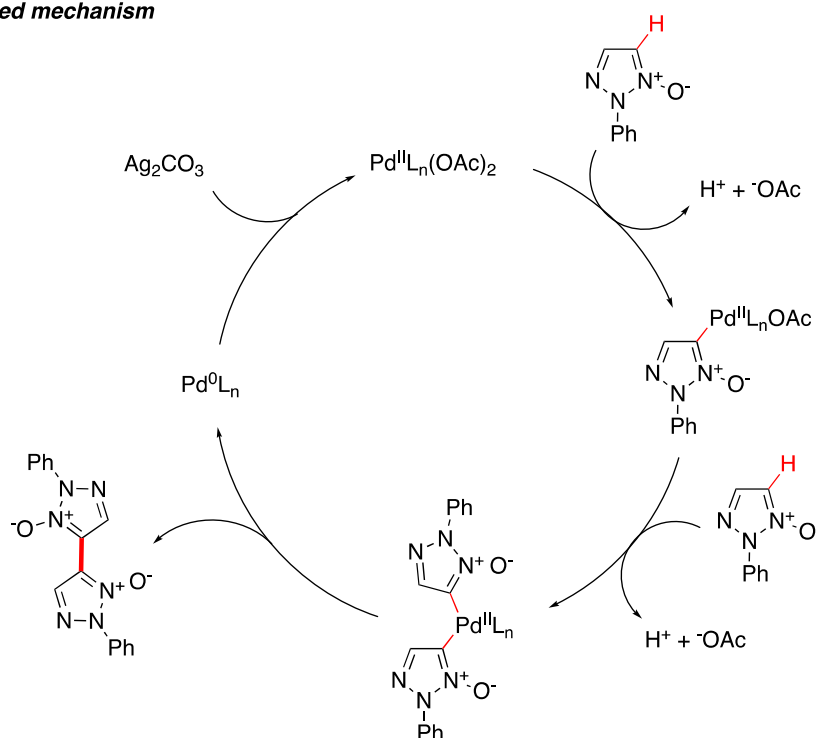
Scheme 8. (**a**) Reaction conditions for the homocoupling of 1,2,3-triazole *N*-oxides in the C4 position through C–H activations using Pd^{II} as the catalyst. (**b**) Suggested mechanism for the homocoupling of 1,2,3-triazole *N*-oxides in the C4 position.

Later, the full scope of the homocoupling reaction between pyrazole-*N*-oxides was investigated by Peng et al. (Scheme 9) [27]. The method showed high regioselectivity towards C–H homocoupling of 1,2,3-triazole *N*-oxides, using a Pd^{II} catalyst (5 mol%), Ag$_2$CO$_3$ and 1,10-phenanthroline under air. Following their previous work, it was found that the addition of the base *t*-BuOK and a catalytic amount of 1,10-phenanthroline allowed for yields of up to 93%.

a) Reaction conditions

R = H, 4-Me, 3-Me, 2-Me, 2,5-Me$_2$, 3,4-Me$_2$,
4-OMe, 2-F, 4-F, 3-Cl, 4-CF$_3$, 2,4-Cl$_2$

b) Substrate scope

85%

83%

77%

68%

79%

80%

63%

86%

88%

93%

90%

86%

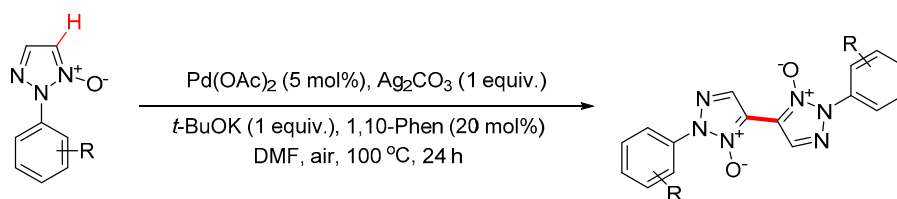**Scheme 9.** (**a**) Reaction conditions for the homocoupling of 1,2,3-triazole *N*-oxides in the C4 position through C–H activations using Pd^{II} as the catalyst. (**b**) Substrate scope of the homocoupling between 1,2,3-triazole *N*-oxides in the C4 position.
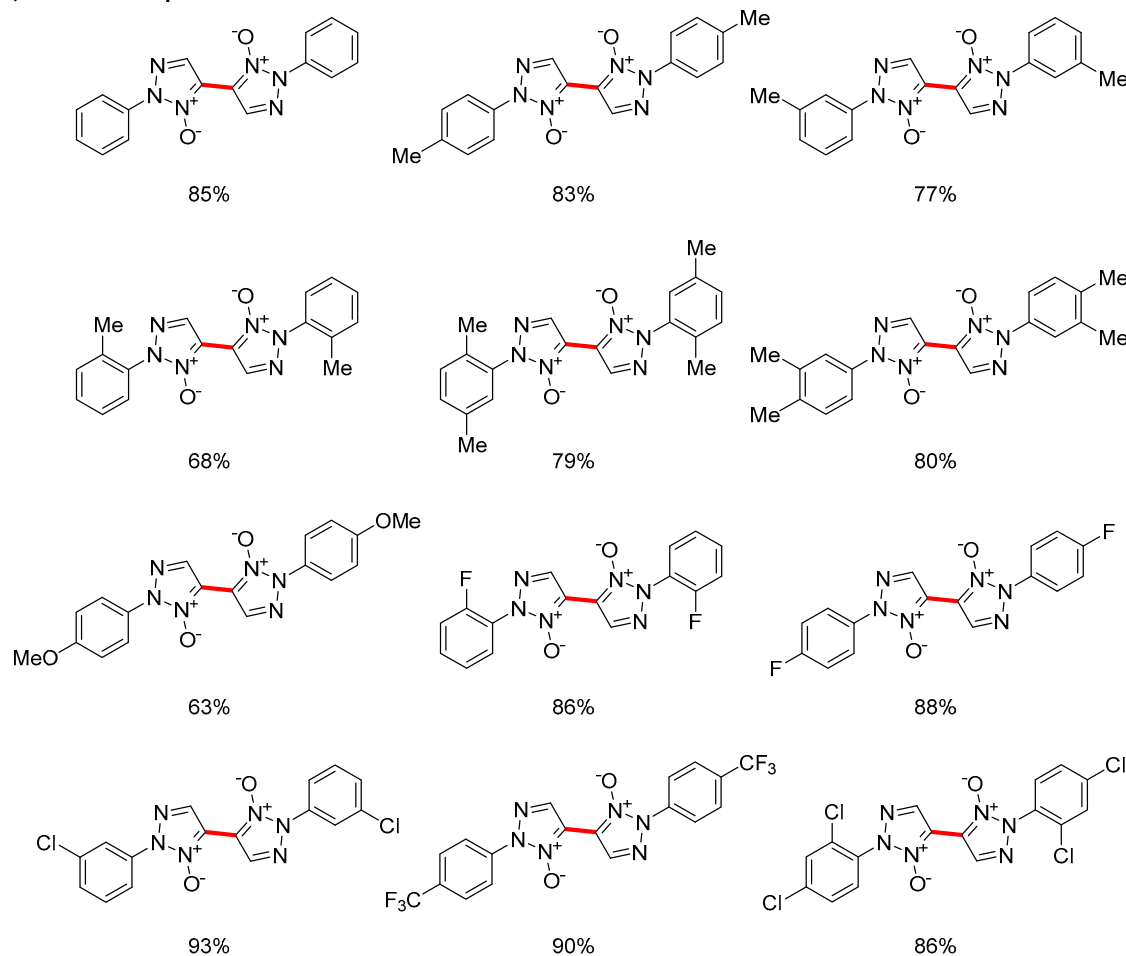
The homocoupling reaction between trisubstituted 4-iodo pyrazoles in the C4 position was investigated by Jansa et al. (Scheme 10) [25]. The pyrazoles contain two to three pyridinyl substituents, which are synthesized from the reaction of 1,3-dipyridinyl-1,3-propanediones with 2-hydrazinopyridine or phenylhydrazine, affording the corresponding 1,3,5-trisubstituted pyrazoles. Iodination at the 4-position of the pyrazoles was achieved by treatment with I$_2$/HIO$_3$. The coupling of two pyrazole rings was achieved under Negishi cross-coupling reaction conditions by employing organozinc halides in combination with a Pd^{II} catalyst.

a) Reaction conditions

b) Suggested mechanism

c) Substrate scope

66%   48%
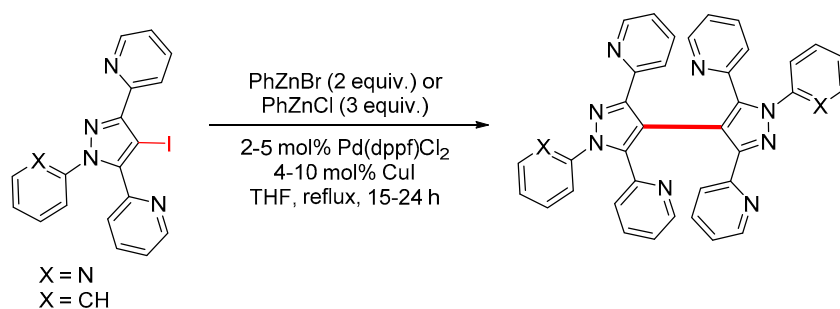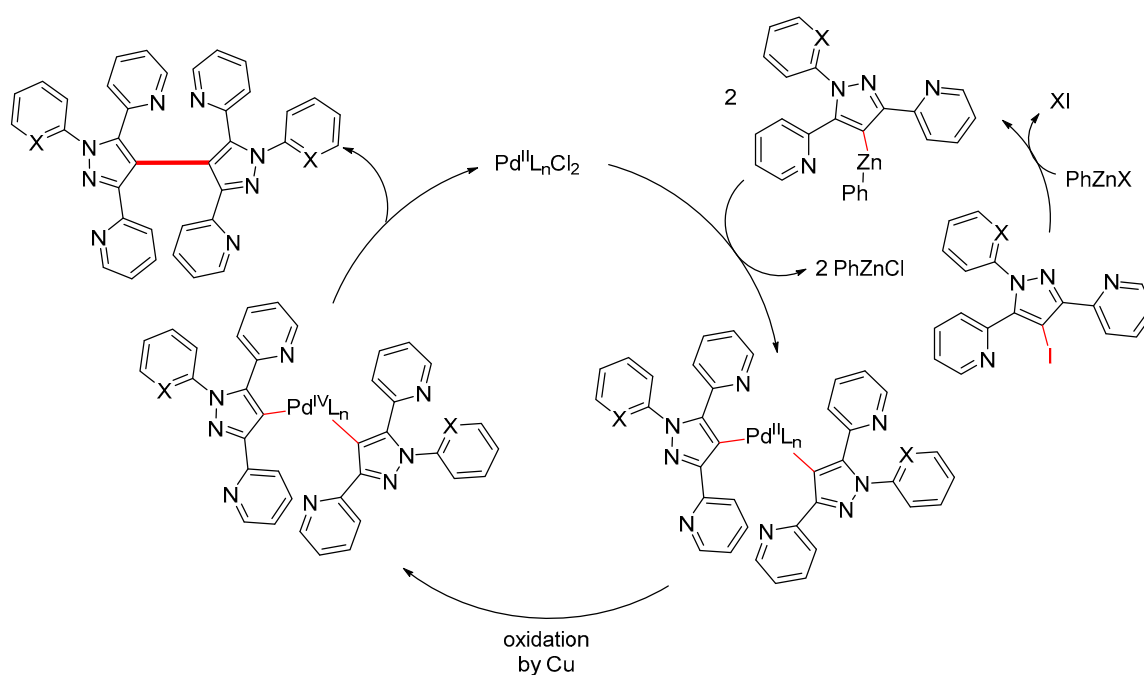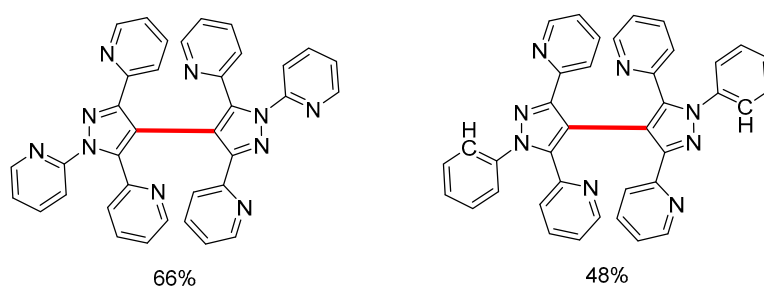
Scheme 10. (**a**) Negishi reaction conditions allows for the homocoupling of 4-iodopyrazoles in the C4 position. (**b**) Suggested reaction mechanism for the Negishi cross-coupling. (**c**) Substrate scope of the homocoupling of 4-iodopyrazoles.

A more recent example of intermolecular homocoupling between two pyrazoles was discovered by Mercedes et al. (Scheme 11): through the palladium-catalyzed homocoupling of pyrazole boronic esters in the presence of air and water, 4,4-bipyrazole (H_2bpz) and other symmetric bipyrazoles could be achieved [28]. The mechanism of the reaction is likely through a Suzuki–Miyaura-type cross-coupling

between the boronic acids (Scheme 11b), with O_2 being the oxidant for the Pd^0 formed during the reductive elimination.

a) Reaction conditions
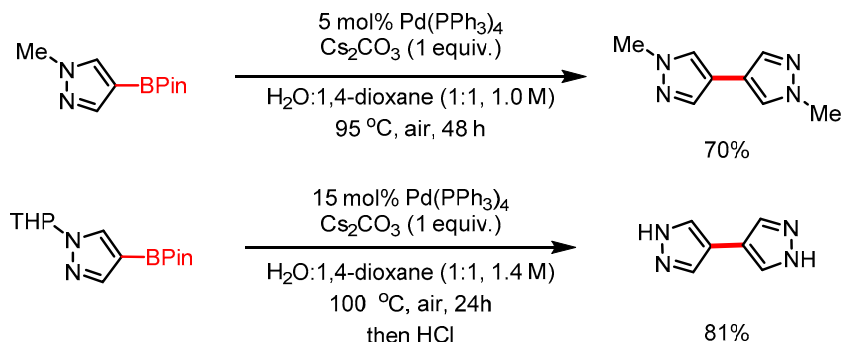
b) Suggested mechanism
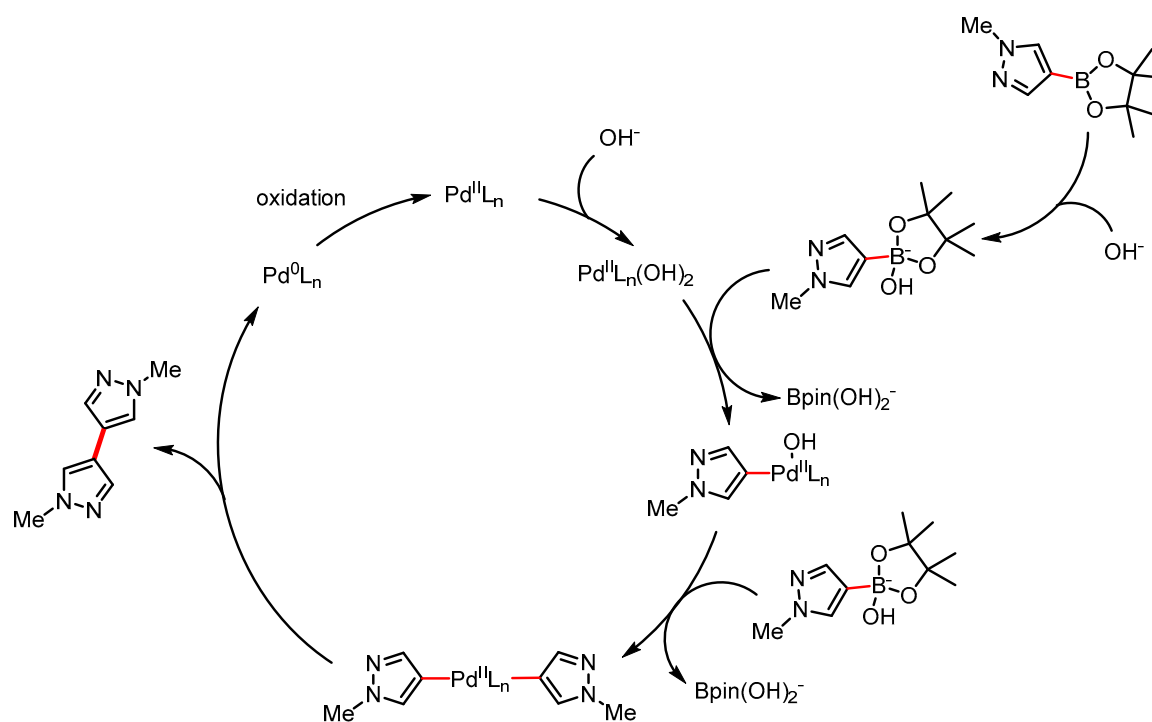
Scheme 11. (**a**) Symmetric bipyrazoles are achieved via the palladium-catalyzed homocoupling of a pyrazole boronic ester in the presence of air and water. (**b**) Suggested mechanism for the homocoupling.

3.1.3. Ru-Catalyzed Homocoupling Reactions

Ackermann et al. demonstrated the chemoselective ruthenium-catalyzed $C(sp^2)$–H bond arylations on triazol-4-yl and pyrazol-2-yl substituted arenes (Scheme 12) [29]. The authors discovered that *ortho*-substituted arenes favored oxidative intermolecular homocoupling reactions to afford dimerized products in high (or moderate) yields. The suggested reaction mechanism follows a double C–H bond activation with carboxylate assistance, followed by reductive elimination.

a) Reaction conditions
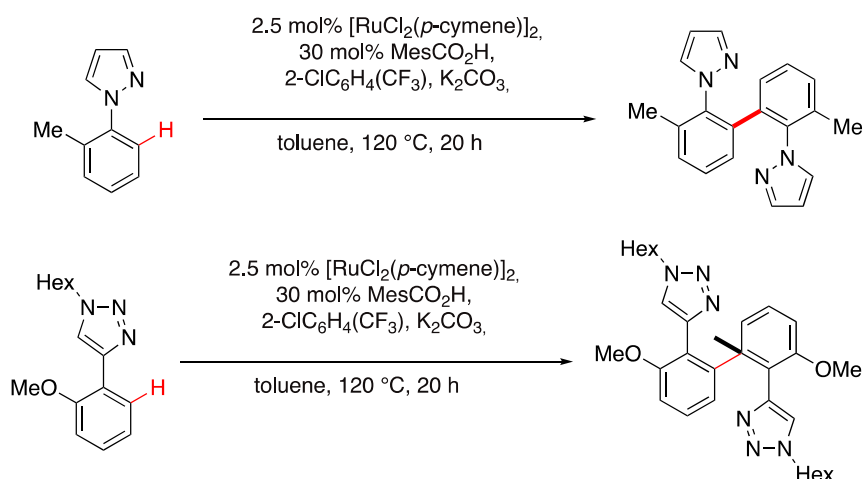
b) Suggested mechanism
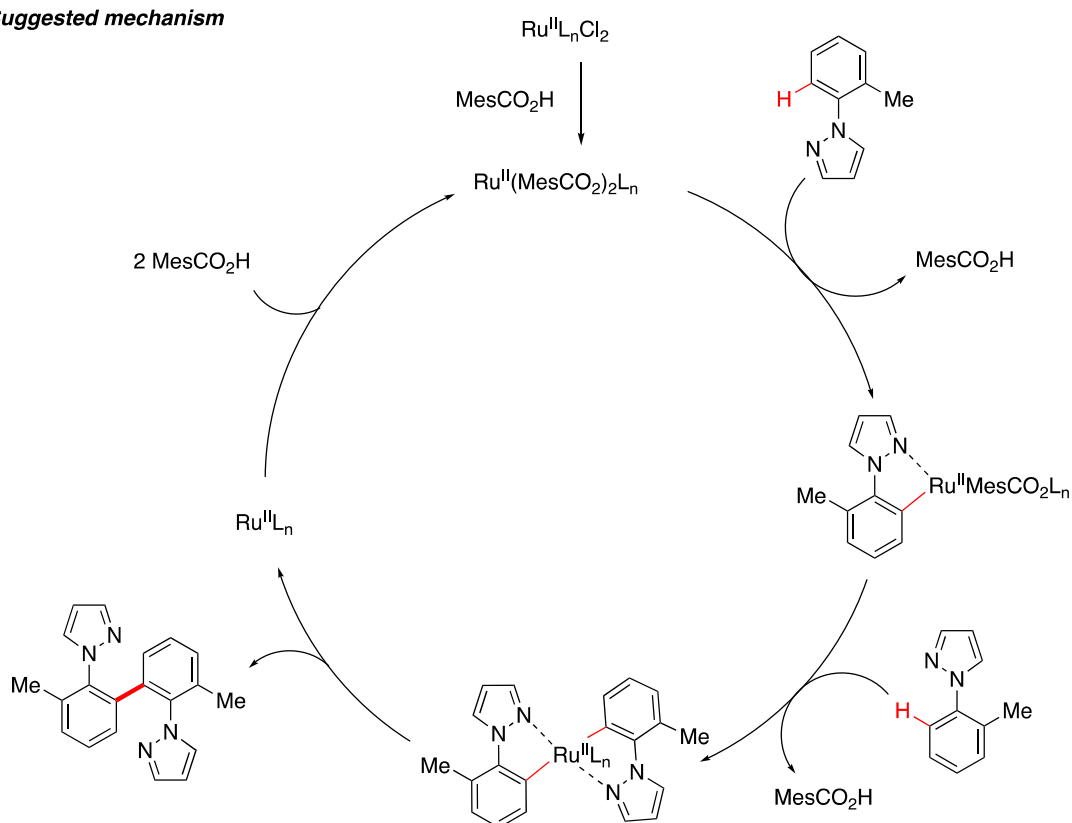
Scheme 12. (**a**) Ruthenium-catalyzed C(sp^2)–H bond activations allows for the homocoupling of triazol-4-yl and pyrazol-2-yl substituted arenes. (**b**) Suggested mechanism for the homocoupling using a Ru^{II} catalyst.

3.1.4. Ni-Catalyzed Reactions

Nickel is an Earth-abundant alternative to Pd and can access various reaction mechanisms, giving a distinct reactivity due to the facile oxidative addition reaction and readily accessible multiple oxidation states [30,31].

In 2000, Fanni et al. reported a new synthetic procedure for the efficient preparation of binuclear Ru(II) polypyridyl complexes, by performing intermolecular homocoupling between two 1,2,4-triazole

bromide in the C3 position (Scheme 13) [32]. The halide functional group is necessary to mediate the Ni-catalyzed reaction in the presence of triphenylphosphine and a zinc reducing reagent.

a) Reaction conditions
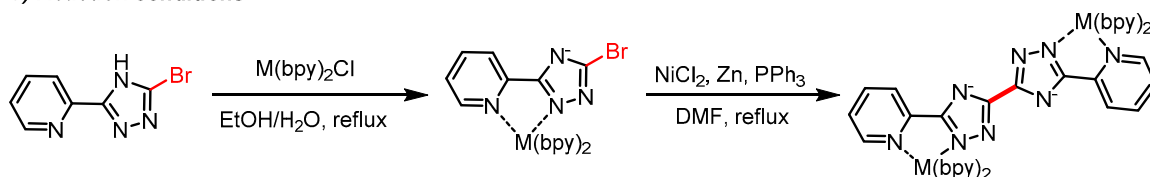
M = Os(II) or Ru(II)

b) Suggested mechanism

c) Substrate scope

8%   8%
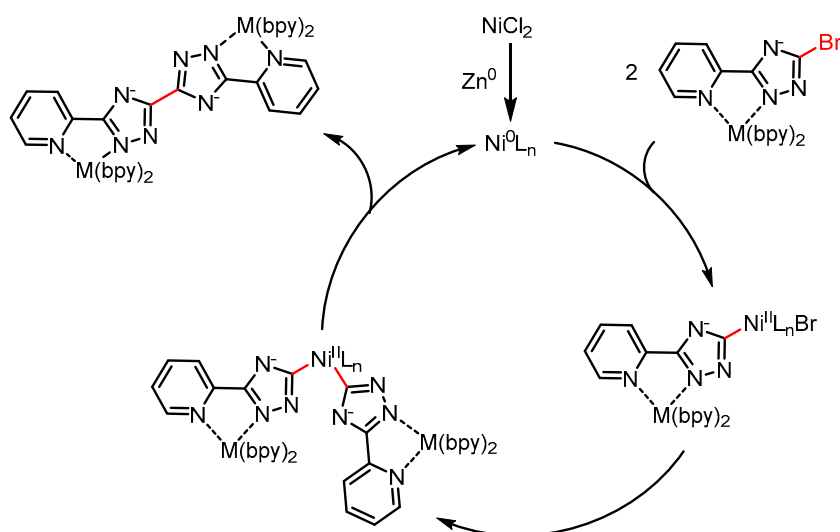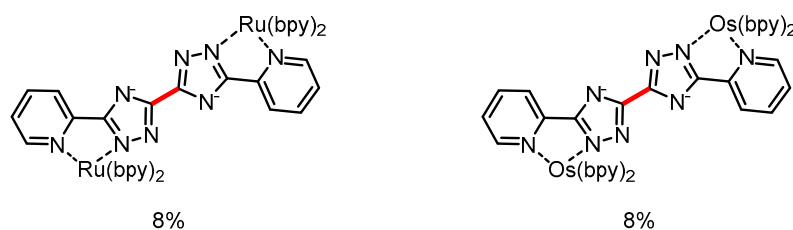
Scheme 13. (**a**) The formation of either ruthenium(II) or osmium(II) complex in water could undergo Ni^0 catalyzed homocoupling from in situ generated Ni^0. (**b**) The mechanism of the homocoupling is suggested to go through double oxidative addition of the 1,2,4-triazole bromides followed by reductive elimination resulting in the homocoupled product. (**c**) Substrate scope for the homocoupling of 1,2,4-triazole bromides in the C3 position.

The homocoupling between 4-bromotriazoles has been reported by Afanas'ev et al. using in situ generated Ni^0 as a catalyst (Scheme 14) [24]. The homocoupling functions via an in situ formation of Ni^0(PPh$_3$)$_4$ from NiCl$_2$ and Zn^0, which undergoes oxidative addition of two equivalents of 4-bromotriazoles, followed by a reductive elimination to form the desired homocoupled products (Scheme 14b).

a) Reaction conditions
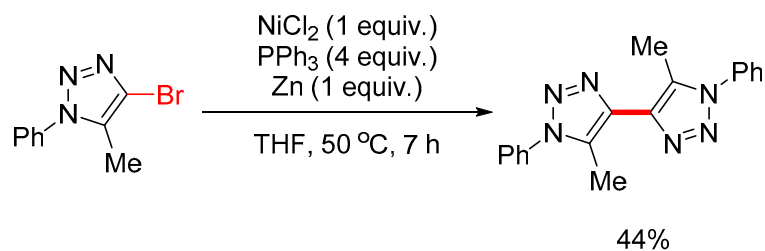
b) Suggested mechanism
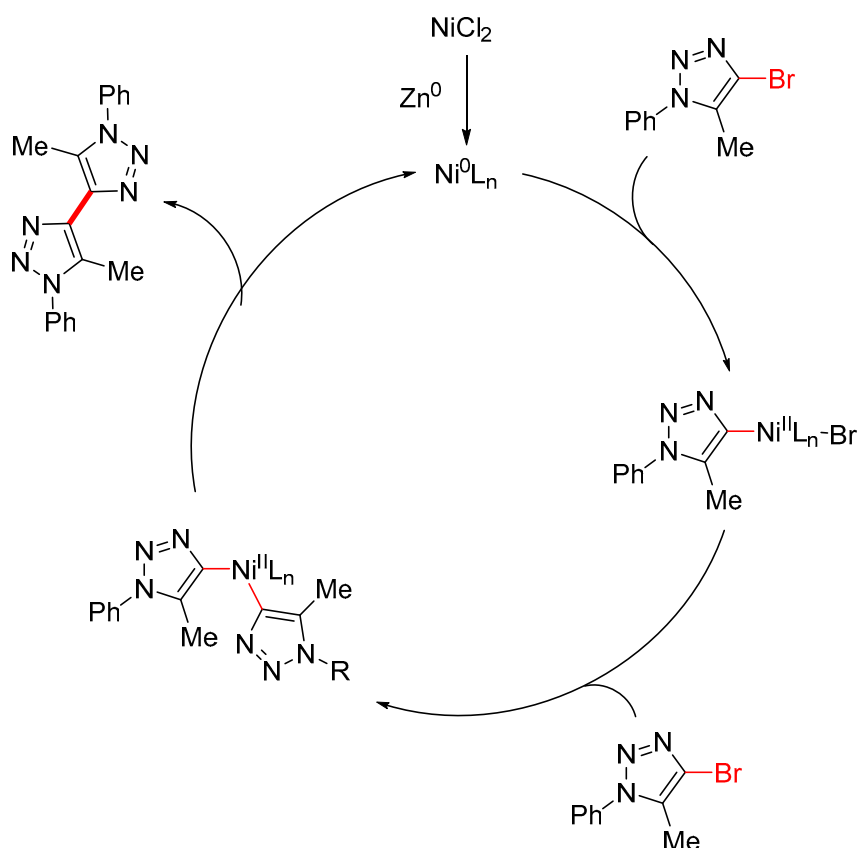
Scheme 14. (**a**) In situ generated Ni^0 used as the catalyst allows for the homocoupling of 4-bromopyrazoles through oxidative addition. (**b**) The mechanism is suggested to go through double oxidative addition of the bromine followed by reductive elimination, resulting in the homocoupled products.

3.1.5. Rh-Catalyzed Homocoupling Reaction

Rhodium-catalyzed reactions have shown fruitful successes in organic reactions [33], particularly in C–H activation and C–C bond formation reactions [34,35]. heterocycle formation reactions [36,37], C–X bond formation reactions [38] and asymmetric synthesis [39].

Yue et al. explored the homocoupling of pyrazole silanes using Rh^I as a catalyst [40]. A suggested reaction mechanism includes a double *trans*-metalation reaction between vinylsilane and a rhodium intermediate in a single catalytic cycle (Scheme 15). While investigating an oxidant, the authors found out hexachloroacetone afforded higher yields of the desired product compared to conventional oxidants such as Cu^{II}, TEMPO and chloranil.

a) Reaction conditions
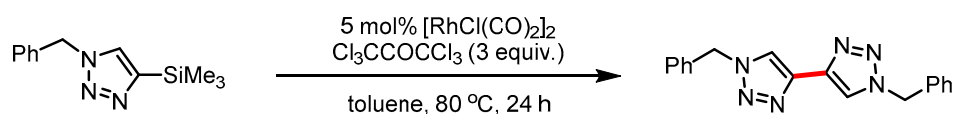
b) Suggested mechanism
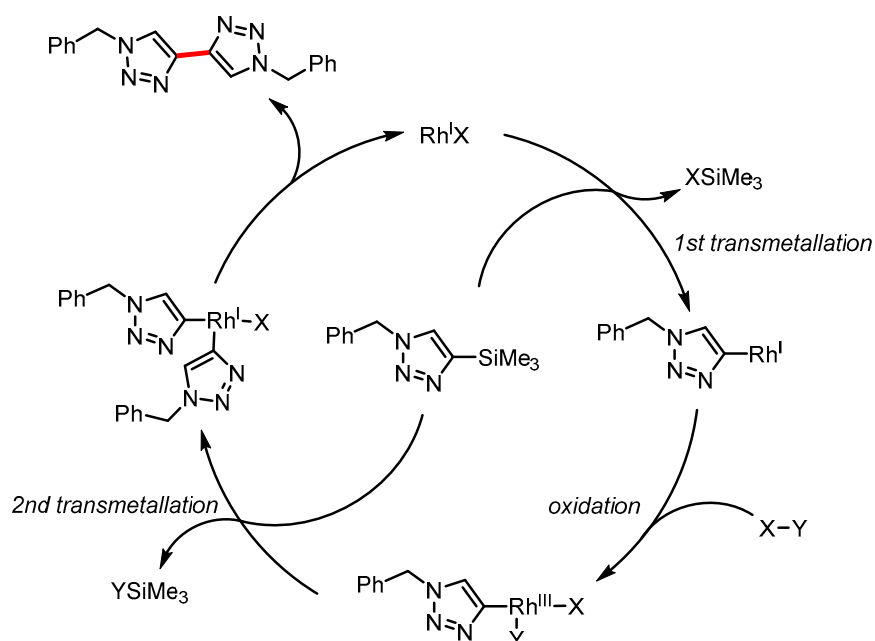
Scheme 15. (**a**) Homocoupling reactions of silane substituted triazoles with catalytic Rh^I. (**b**) Suggested mechanism for the homocoupling of silane substituted triazoles.

3.1.6. Fe-Catalyzed Homocoupling Reactions

Iron is one of the most Earth-abundant metals, and many iron complexes are commercially available. Surprisingly, despite its many advantages, iron has been relatively underrepresented in the catalysis of organic compounds until recently, compared to other transition metals.

In 2010, Luque et al. achieved the homocoupling of two pyrazole boronic acids utilizing nano-ferrite glutathione in a microwave (MW)-assisted aqueous reaction, providing an alternative to the palladium-catalyzed Suzuki coupling reaction (Scheme 16) [41].
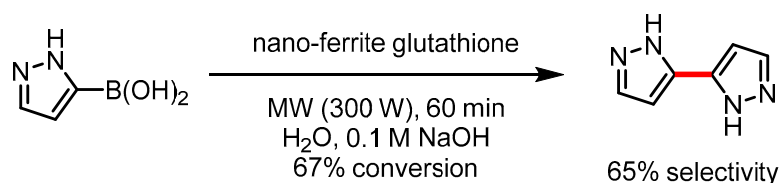
Scheme 16. The homocoupling of boronic acid substituted pyrazoles is possible when nanoparticles of iron are used as the catalyst in water under microwave conditions.

3.2. Metal-Free Homocouplings of Azoles

In addition to the many transition metal-catalyzed routes described above, azole substrates have also been shown to undergo homocoupling reactions in the absence of a metal catalyst. Hypervalent iodine reagents can induce aryl–aryl bond formation in a wide variety of substrates, including pyrroles,

pyrazoles, imidazoles and triazoles, as has been recently reviewed [42]. Other approaches to metal-free couplings rely on oxidants or photocatalysis to enact radical-mediated dimerizations. Some recent examples are presented below.

There is precedent for the metal-free homocoupling of pyrazolones through the use of oxidants like phenoxy radicals [43] or O_2 [44]. A recent example extends this approach to a switchable aerobic oxidation, in which a pyrazol-5-one starting material undergoes either hydroxylation or a homocoupling, using O_2 as an oxidant (Scheme 17a) [45]. Simple changes in reaction conditions control the outcome of this reaction; oxidation in dioxane in the presence of base favors hydroxylation, whereas a base-free reaction in acetonitrile favors the homocoupling. The homocoupling reaction was successful for 19 different substrates containing various substituents at positions R^1 and R^2, in yields up to 77% (Scheme 17b). Most reactions led to a mixture of diastereomers, with diastereomeric ratios ranging from 3.1:1 to 5.7:1, although three substrates led to a single diastereomeric product. The authors hypothesize that the homocoupling reaction proceeds through a radical intermediate, although mechanistic studies were not undertaken for this reaction.
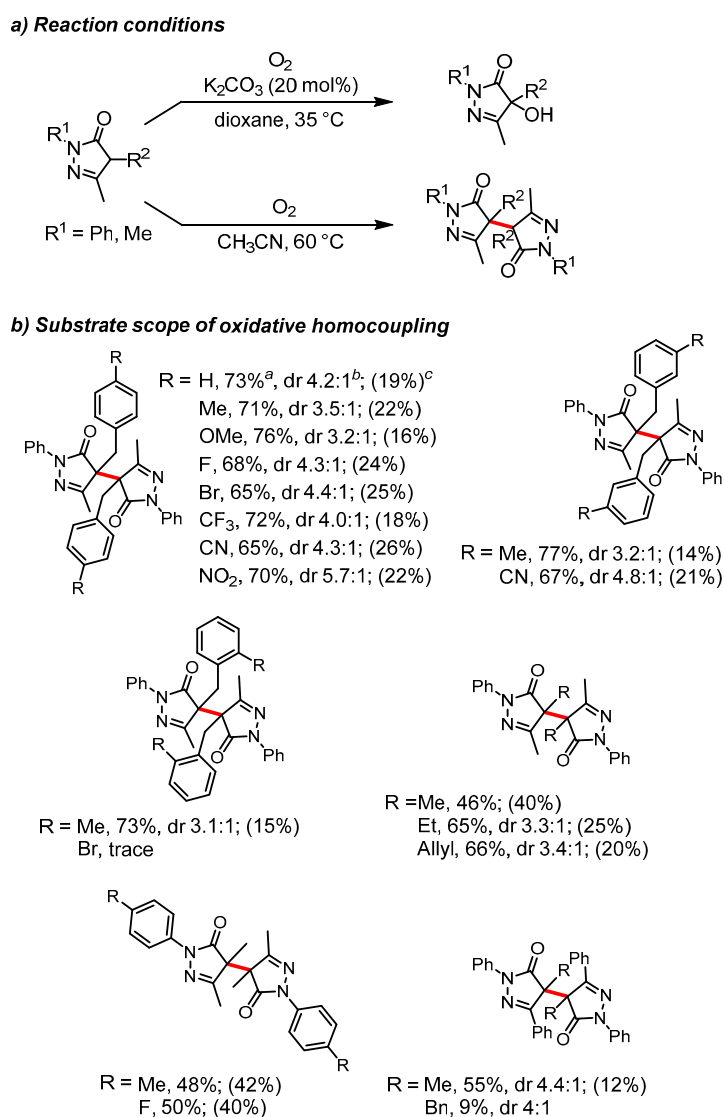
Scheme 17. (**a**) A switchable aerobic oxidation of a pyrazol-5-one results in either hydroxylation or homocoupling, depending on reaction conditions. (**b**) Substrate scope of the oxidative homocoupling. [29]. [a] Isolated yields. [b] The dr values were determined by ^{1}H-NMR. [c] Isolated yield of hydroxylated products.
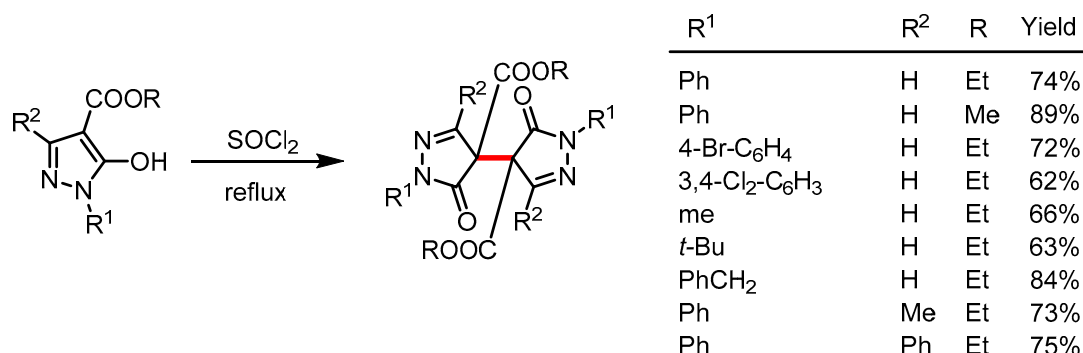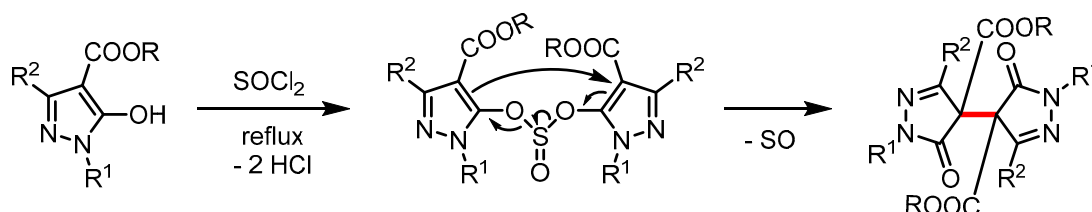
Another homocoupling reaction was recently shown to yield a structurally similar bipyrazolone, but through remarkably different conditions: By refluxing a substituted pyrazole in excess thionyl chloride, the bipyrazolone was produced in high yields (Scheme 18a) [46]. This reaction was successful for nine substrates in yields from 62–89%. (The authors do not provide diastereomeric ratios of meso compounds and racemate for each substrate, but they report that dimeric pyrazolone (R^1 = Ph) appeared to be a racemic mixture by ^{1}H-NMR spectroscopy and X-ray crystallography). The reaction was shown to proceed under an atmosphere of N_2 and under air, ruling out oxidation by air as the mechanism, and the authors propose a hypothetical mechanism via a di(pyrazolyl) sulfite intermediate (Scheme 18b).

a) Reaction conditions and substrate scope

R^1	R^2	R	Yield
Ph	H	Et	74%
Ph	H	Me	89%
4-Br-C_6H_4	H	Et	72%
3,4-Cl_2-C_6H_3	H	Et	62%
me	H	Et	66%
t-Bu	H	Et	63%
$PhCH_2$	H	Et	84%
Ph	Me	Et	73%
Ph	Ph	Et	75%

b) Proposed mechanism

Scheme 18. (**a**) Reaction conditions and substrate scope for the thionyl chloride-mediated homocoupling of substituted pyrazolones. (**b**) The reaction is proposed to proceed via a di(pyrazolyl) sulfite intermediate.

Two recent reports describe the oxidative homocoupling of 4-amino-1,2,4-triazoles, yielding the corresponding symmetrical bis(triazoles). Yang and coworkers used the oxidant α-hydroxy-α-methylthioacetophenone to accomplish the homocoupling of five substituted 4-amino-1,2,4-triazoles in yields of 59–73% (Scheme 19a) [47]. Likewise, Zhao and coworkers accomplished the homocoupling of the unsubstituted 4-amino-1,2,4-triazole in 90% yield using sodium dichloroisocyanurate (SDCI) as the oxidant (Scheme 19b) [48].

Photocatalysis represents an alternative metal-free approach to pyrazole homocouplings. An early report of the photochemical oxidation of pyrazolidinones led to a homocoupled product [49]. More recently, Meng and coworkers used photocatalysis to accomplish the homocoupling of a bromopyrazolone [50]. By irradiating a solution of 4-bromo-3-methyl-1-phenyl-4,5-dihydropyrazol-5-one (PyHBr) and naphthalene in acetonitrile with a 300 W high-pressure mercury lamp, the authors obtained the homocoupled product in 64% yield (Scheme 20a). Interestingly, the authors discovered that by substituting phenathrene for naphthalene the dehydrogenated product was favored over the hydrogenated product, and the use of other arenes such as anthracene, benzene, acenaphthylene or indole did not lead to homocoupling at all. As the reaction relies on certain arenes and does not proceed

under UV irradiation alone, the authors ruled out the homolytic bond cleavage of the carbon–bromine bond as the mechanism and instead proposed the mechanism shown in Scheme 20b.

a) Reaction conditions and substrate scope

R = CH₃ (65%)

R = CH₂CH₃ (70%)

R = (phenyl) (59%)

R = (4-OCH₃-phenyl) (68%)

R = (4-CF₃-phenyl) (73%)
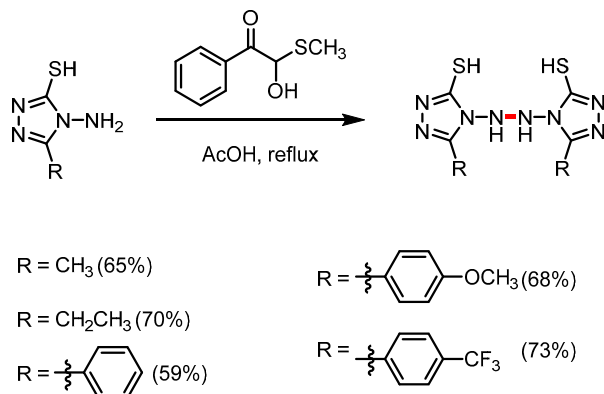
b) Reaction conditions
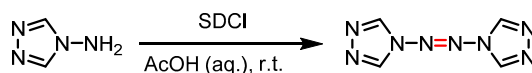
Scheme 19. (**a**) Reaction conditions and substrate scope for the oxidative homocoupling of substituted 4-amino-1,2,4-triazoles. (**b**) Reaction conditions for the homocoupling of unsubstituted 4-amino-1,2,4-triazole.

a) Reaction conditions

64%

41%   +   29%

b) Proposed mechanism

PyHBr + ArH ⟶ [PyHBr---ArH]· ⟶ [PyHBr·⁻---ArH·⁺]
                Exciplex   Radical ion pair

PyHBr·⁻ ⟶ PyH· + Br⁻

2 PyH· ⟶ HPy—PyH

HPy—PyH + 2ArH·⁺ ⟶ Py=Py + 2ArH + H⁺
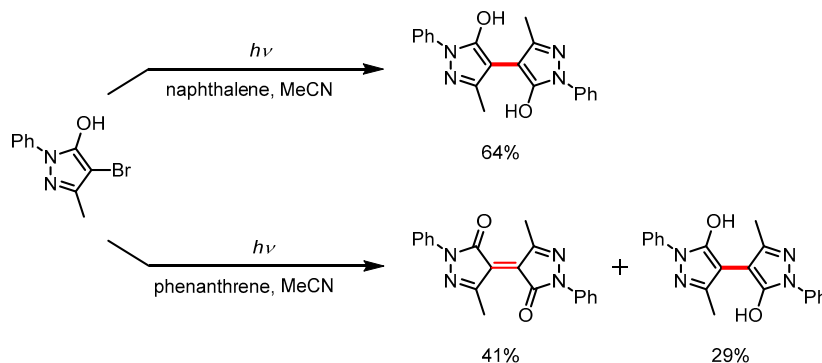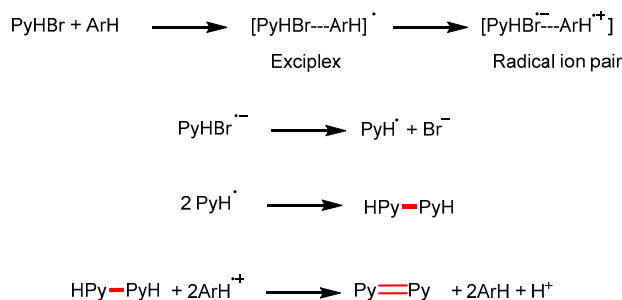
Scheme 20. (**a**) Photochemical oxidation of pyrazolidinones leads to different products depending on the identity of the auxiliary arene (naphthalene vs. phenanthrene). (**b**) The proposed reaction mechanism reflects the fact that UV irradiation alone is not sufficient to catalyze the homocoupling [34].

Finally, a recent report of the decarboxylative fluorination of various heterocycles using Selectfluor contained the unexpected observation of homocoupling under certain conditions [51]. Specifically, substituted pyrazole-5-carboxylic acids and indole-2-carboxylic acids underwent homocoupling along with decarboxylative fluorination, yielding the corresponding fluorinated dimers (Scheme 21a). The homocoupling occurred in high yields (70–82%) for the pyrazole-based substrates and in moderate yields (38–58%) for the indole-based substrates (Scheme 21b). In the case of indole-2-carboxylic acid, the biproducts 2-fluoroindole and oxindole were generated along with the dimer (Scheme 21c). Mechanistic investigations indicated that neither of these biproducts is an intermediate in the dimer formation process, but the mechanism of the homocoupling was not elucidated.

a) Reaction conditions
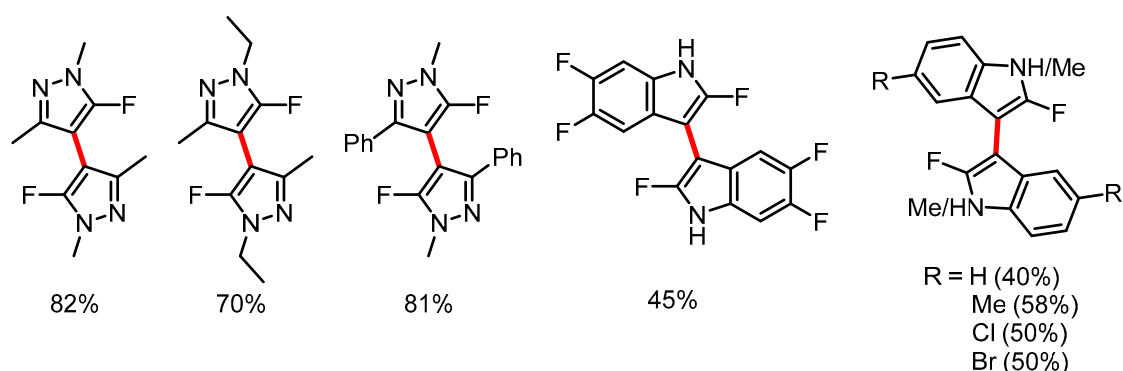
b) Substrate scope

c) Byproducts of indole-2-carboxylic acid homocoupling

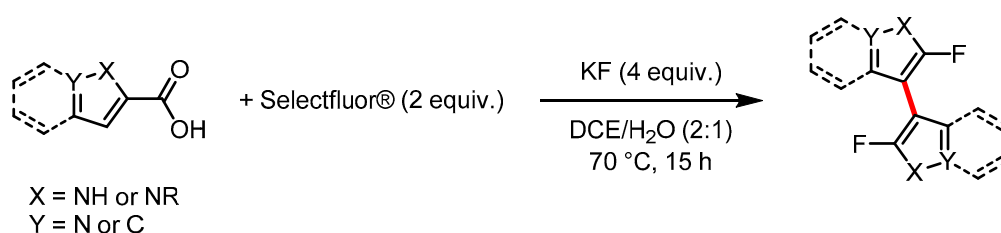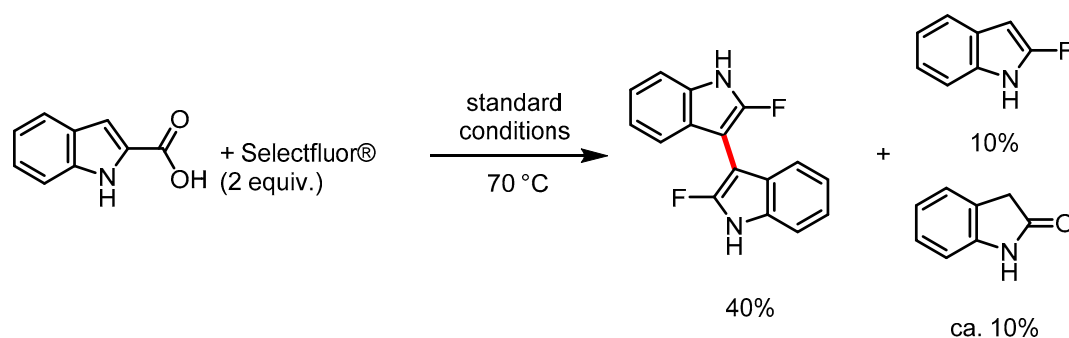**Scheme 21.** (**a**) Reaction conditions for the homocoupling and decarboxylative fluorination of heterocycles in the presence of Selectfluor. (**b**) Substrate scope for the homocoupling of substituted pyrazoles and indoles using these conditions. (**c**) The homocoupling of indole-2-carboxylic acid led to the formation of byproducts and the dimer.

3.3. Applications in MOFs

The pyrazole functional group can coordinate with a transition metal as a ligand through the lone pair on the non-protonated nitrogen atom (Figure 2a) [52,53]. When the other nitrogen

atom in the ring is deprotonated (to yield the pyrazolate), both nitrogen atoms can coordinate with metals, allowing pyrazolate to bridge metal centers and give rise to clusters, chains or coordination polymers (Figure 2b) [54,55]. Bipyrazolate ligands can coordinate up to four different metal centers (Figure 2c), making possible the construction of extended three-dimensional structures known as metal–organic frameworks (MOFs) [56]. Due to their crystallinity and internal porosity, metal–organic frameworks have shown promise in diverse applications, including gas separations [57], sensing [58], conductivity [59], drug delivery [60] and energy storage [61]. Numerous metal–organic framework structures have been designed and synthesized using poly(pyrazole) ligands as building blocks, as was reviewed by Galli and coworkers in 2016 [62]. Here we give an overview of recent studies on pyrazole-based metal–organic frameworks that have been published since the 2016 review, with an emphasis on 4,4′-bipyrazole (H_2bpz) and its derivatives.
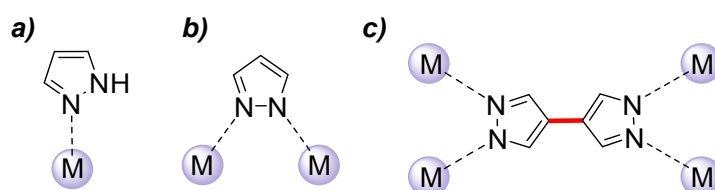
Figure 2. The pyrazole functional group can coordinate with a single metal ion (**a**) or can bridge two metal ions as a deprotonated pyrazolate (**b**). The 4,4′-bipyrazolate ligand can coordinate up to four different metal ions (**c**).

The unsubstituted H_2bpz ligand has recently been used to form two new metal–organic frameworks (Figure 3). Volkmer and coworkers reacted H_2bdp with a mixed-valent iron precursor to yield a nonporous metal–organic framework with Fe(II) ions as the framework nodes (CFA-10-as), and the authors were then able to convert the framework to a porous form upon thermal treatment (CFA-10) [63]. This single-crystal-to-single-crystal transformation was shown to result from the thermal decomposition of formate ions in the pores of CFA-10-as, resulting in a final porous structure that could not be achieved directly through solvothermal synthesis. A subset of these authors also described the synthesis of another H_2bpz-based metal–organic framework, this time with Mn(III) ions as the framework nodes [64]. The structure of this framework, named Mn-CFA-6, was shown to contain two crystallographically and structurally distinct manganese centers, and the framework exhibited structural flexibility in response to the removal of guest molecules. Recently, Lee and coworkers observed a similar flexibility in the H_2bpz-based framework Co(bpz), which undergoes reversible structural changes in response to gas adsorption or temperature change [28].

Figure 3. H_2bpz was reacted with an iron source to yield CFA-10-as and CFA-10 [47] and with a manganese source to yield Mn-CFA-6. Adapted with permission from references [63,64]. ©2017 ACS.

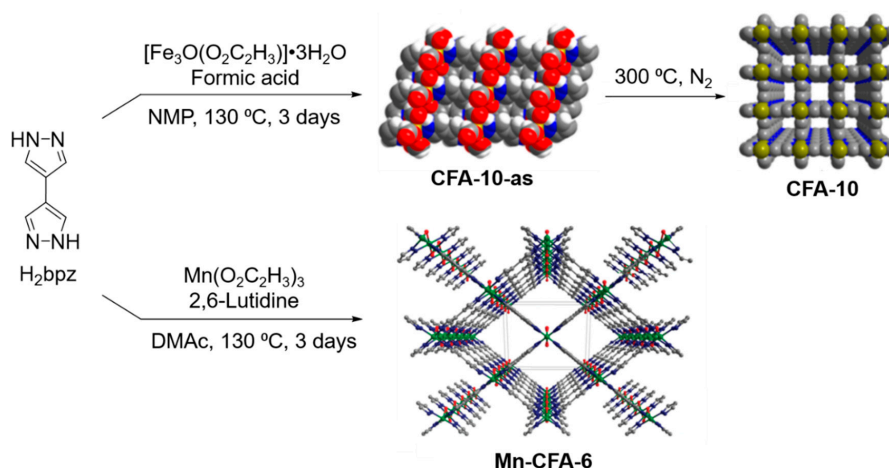The tetramethylated bipyrazole ligand, 3,3',5,5'-tetramethyl-4,4'-bipyrazole (H$_2$Me$_4$bpz), is another popular building block for metal-organic frameworks. In 2015, Sun and coworkers used H$_2$Me$_4$bpz to construct a series of Cu(I)-based coordination networks, including two novel metal–organic frameworks (Figure 4) [65]. These two frameworks contain halide and cyanide anions that coordinate with the Cu(I) nodes, along with the Me$_4$bpz^{2-} ligands. The authors investigated these materials as heterogeneous catalysts for the azide–alkyne click reaction, because of the high density of Cu(I) sites present in the frameworks, by reacting benzyl azide with phenylacetylene in the presence of 1 mol % of a given metal–organic framework. The frameworks proved to be very effective catalysts for the formation of the substituted triazole, with the framework [Cu$_6$(Me$_4$bpz)$_6$ (CH$_3$CN)$_3$(CN)$_3$Br]•2OH•14CH$_3$CN leading to a 99% yield within 2 h. The authors ascribed this excellent catalytic performance to the framework's high porosity and large pore diameter, which allow the Cu(I) active sites to be accessible to the reactants. The substrate scope for compound [Cu$_6$(Me$_4$bpz)$_6$ (CH$_3$CN)$_3$(CN)$_3$Br]•2OH•14CH$_3$CN was shown to include a variety of terminal azides and alkynes. This work was the first investigation of Cu(I)-based metal–organic frameworks as catalysts for click reactions, and the results indicate that this class of materials holds great promise in heterogeneous azide–alkyne catalysis.
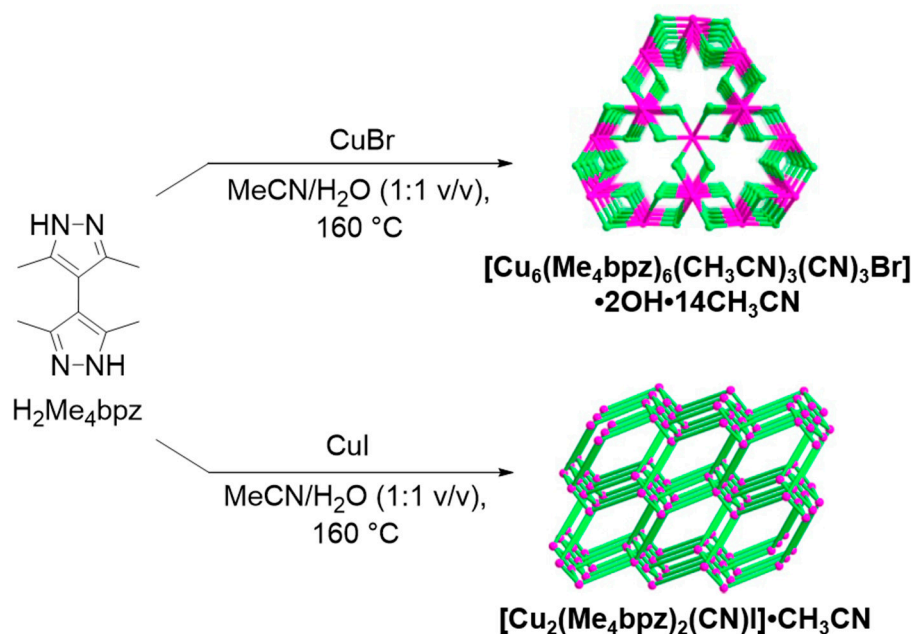
Figure 4. H$_2$Me$_4$bpz was reacted with Cu(I) halides to yield two Cu(I)-based metal–organic frameworks, which were shown to be effective catalysts for azide–alkyne click reactions. Adapted with permission from reference [65]. ©2015 ACS.

Chen and coworkers attempted to increase the hydrophobicity of the hallmark metal–organic framework MOF-5 by substituting the traditional 1,4-benzenedicarboxylic acid (H$_2$bdc) ligand with combinations of H$_2$Me$_4$bpz, naphthalene-1,4-dicarboxylic acid (H$_2$ndc) and biphenyl-4,4'-dicarboxylic acid (H$_2$bpdc) [66]. The authors synthesized one known framework (MAF-X10) and two new frameworks (MAF-X12 and MAF-X13) from these building blocks (Figure 5). The three metal–organic frameworks were investigated for fluorocarbon adsorption, using CHClF$_2$ as a representative adsorbate, and all three were shown to possess high adsorption capacities for CHClF$_2$. Grand canonical Monte Carlo simulations indicated that the strongest CHClF$_2$ binding site in each framework was located in a hydrophobic pocket formed by two methyl groups from Me$_4$bpz^{2-} ligands and the aromatic face of an adjacent phenyl ring, bearing out the authors' hypothesis that increased ligand hydrophobicity would be beneficial for fluorocarbon adsorption. The compound MAF-X13 was shown to have the

largest saturation uptake and the largest working capacity for $CHClF_2$ adsorption, due to its type-IV isotherm shape.

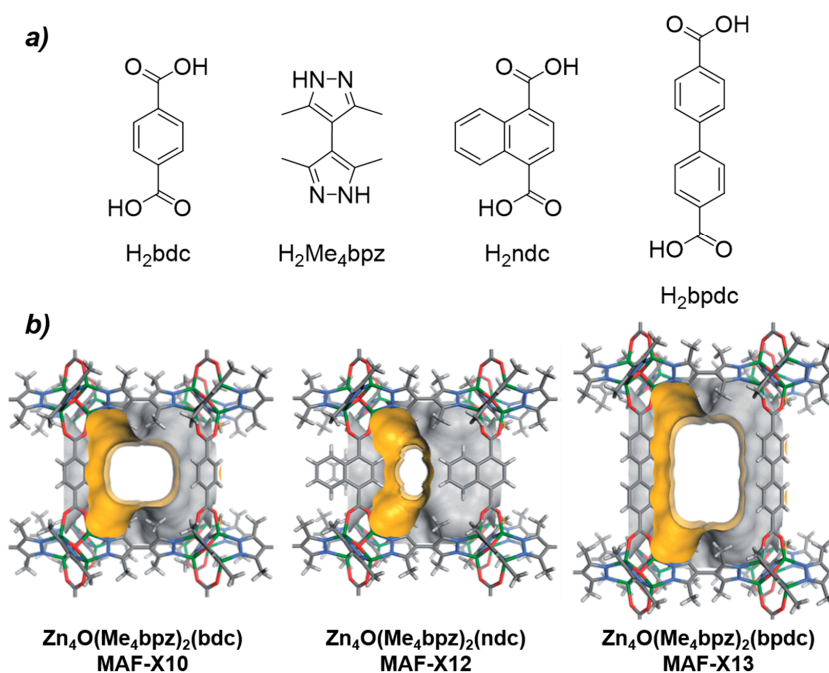**Figure 5.** (**a**) Linkers used to make hydrophobic MOF-5 analogues. (**b**) Crystal structures of MAF-X10, MAF-X12 and MAF-X13 highlighting the pore surface. Adapted with permission from ref. [66].

Recently, Cao and workers took advantage of the differences in dative bond strength between carboylate ligands and azolate ligands to partially deconstruct mixed-ligand metal–organic frameworks [67]. The authors synthesized a metal–organic framework from a Zn(II) source and a mixture of H_2Me_4bpz and 1,4-benzenedicarboxylate ligands, and then used a pH 13 ammonia solution to dissolve the Zn–carboxylate bonds but not the Zn–pyrazolate bonds. This treatment led to a delamination of the three-dimensional framework, yielding two-dimensional sheets composed of Zn(II) nodes linked by $Me_4bpz_2{}^-$ ligands. The authors also applied this process to an analogous Zn–triazolate–thiophenedicarboxylate MOF and used the resulting 2D Zn–triazolate sheets as building blocks to construct a library of new 3D frameworks, by combining the 2D sheets with various dicarboxylate linkers (Figure 6). This creative approach to metal–organic framework synthesis highlights the advantages of the strong metal–ligand bonding inherent to bipyrazole ligands like H_2Me_4bpz.
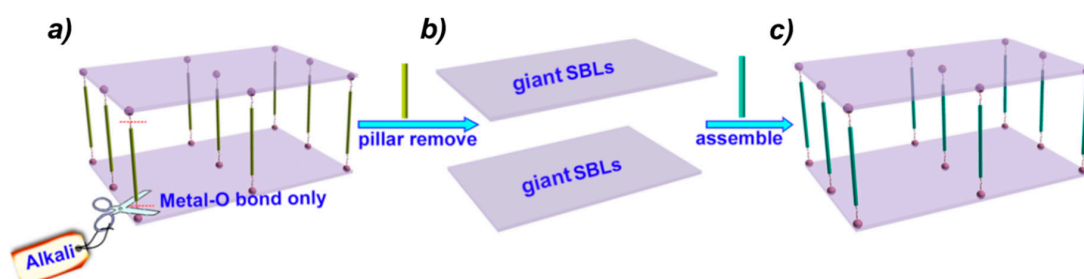
Figure 6. (**a**) A metal–organic framework composed of sheets of Zn–azolate bonds pillared by Zn–carboxylate bonds undergoes alkaline treatment to break the Zn–carboxylate bonds only. (**b**) This treatment leaves behind Zn-azolate sheets, which can be thought of as giant supramolecular building layers (SBLs). (**c**) These layers can then be reassemble using different dicarboylate pillars to yield a variety of metal–organic frameworks. Adapted with permission from reference [67]. ©2015 ACS.

The sheer number of other recent examples of H_2Me_4bpz-based metal–organic frameworks emphasizes the utility of this bipyrazole ligand. These frameworks combine H_2Me_4bpz with various transition metals, including manganese [68], iron [69], cobalt [68,70,71], nickel [68], copper [72] zinc [73], silver [74–76] and cadmium [68,77,78], yielding a diverse array of framework topologies and functionalities. These frameworks were investigated for applications ranging from antibacterial therapy [76] to the photocatalytic degradation of organic pollutants [71], and chemists are sure to push the boundaries of H_2Me_4bpz-based metal–organic frameworks further in the coming years.

The dimethylated analogue of H_2bpz is used in metal–organic framework synthesis less frequently than the tetramethylated analogue, but two recent studies show that H_2Me_2bpz can be used to form a variety of metal–organic frameworks. In 2017, Galli and workers reported two new metal–organic frameworks based on the reaction of H_2bpz with a cobalt source and with a zinc source, respectively (Figure 7a). [79] The authors compared these two H_2Me_2bpz frameworks with the isostructural frameworks M(bpz) (M = Co, Zn) through techniques including gas adsorption and *ab initio* simulation, revealing that the methylated frameworks bound guest CO_2 molecules more strongly than the nonmethylated frameworks but accommodated fewer overall guests because of the increased steric bulk of the H_2Me_2bpz ligand, relative to H_2bpz. Additionally, in 2018 a subset of these authors reported a 3D polymeric network composed of Hg(II) ions linked by $Me_2bpz_2^-$ ligands (Figure 7b). [80]
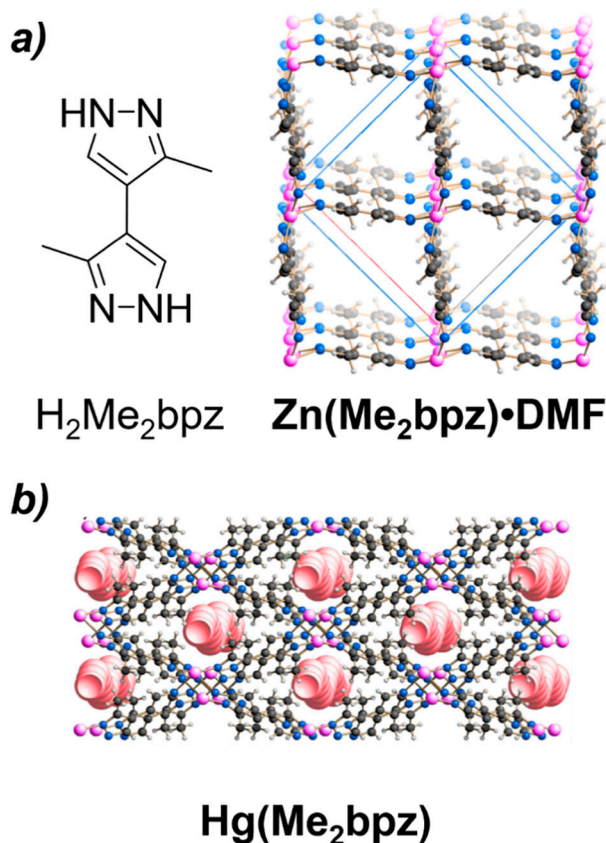
Figure 7. (**a**) The H_2Me_2bpz ligand and the resulting metal–organic framework Zn(Me₂bpz)•DMF (DMF = *N,N*-dimethylformamide). DMF molecules in the pores have been removed for clarity. Co(Me₂bpz) •DMF is isostructural to Zn(Me₂bpz)•DMF. Adapted with permission from reference [79]. ©2017 ACS. (**b**) The 3D polymeric network Hg(Me2bpz), with the void spaces highlighted. Adapted with permission from reference [80].

Finally, Galli and coworkers recently demonstrated the power of introducing functional groups onto the H_2bpz scaffold, functionalizing this ligand with either NO_2 or NH_2 groups (Figure 8a) [81]. The authors incorporated these H_2bpz derivatives into a series of Zn(II)-based metal–organic

frameworks, each containing a different mixture of ligands. The authors found that frameworks containing a mixture of H_2bpz and H_2bpzNH_2 ligands had the best gas adsorption properties in the context of N_2/CO_2 separations. The following year, Rossin and coworkers used the same three ligands to construct a series of Co(II)-based metal–organic frameworks (Figure 8b) [82]. The authors found that while the unfunctionalized Co(bpz) had higher O_2 gas uptake relative to Co(bpzNO$_2$) and Co(bpzNH$_2$), ligand functionalization could tune the catalytic selectivity and performance of these materials when they were used for cumene oxidation and decomposition.
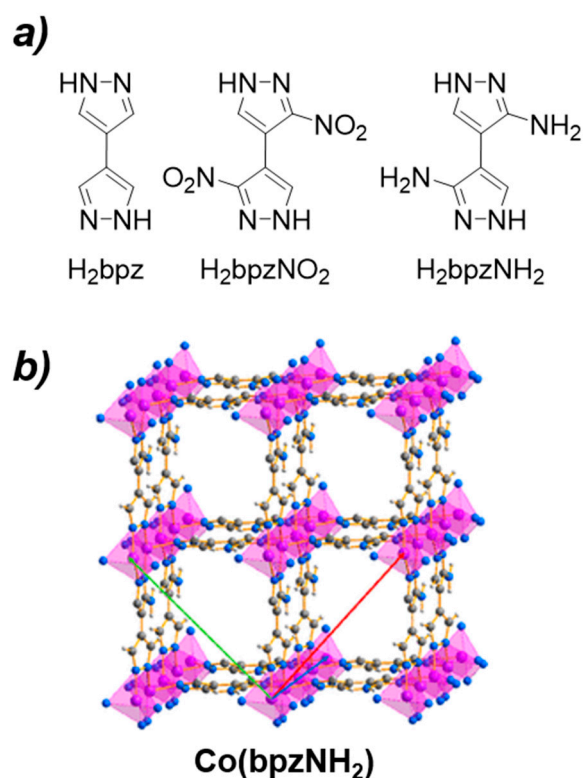

Figure 8. (**a**) The series of H_2bpz derivatives. (**b**) Crystal structure of Co(bpzNH$_2$), which is isostructural to Co(bpz) and Co(bpzNO$_2$). Adapted with permission from reference [81]. ©2019 ACS.

4. Conclusions

Despite the utility of bipyrazoles and other symmetric heterocycles as building blocks in coordination chemistry, traditional routes to these molecules were laborious, multi-step syntheses with poor atom economy and redox efficiency. In recent years, a number of improved routes to bipyrazoles have been published, employing an efficient homocoupling step that forms an aryl-aryl bond between the two halves of the product. Some of the most promising pyrazole homocoupling reactions rely on transition metal catalysts, especially palladium, as described above. We have also described other unique homocoupling strategies that proceed in the absence of metal catalysts, relying on UV irradiation, aerobic oxidation, or other diverse mechanisms.

We anticipate that the coupling strategies provided in this review will allow metal–organic framework chemists to access a greater variety of bipyrazole-type ligands, beyond the small set of H_2bpz derivatives described herein. As is obvious from the above studies, bipyrazole-based metal–organic frameworks are promising materials for a number of applications, especially gas adsorption and heterogeneous catalysis. The ability to diversify and functionalize bipyrazole ligands will afford chemists greater control over the resultant metal–organic framework properties, leading to even better adsorbents and catalysts.

References

1. Hab, D.; Mlostoń, G. Heterocycles in materials chemistry. *Chem. Heterocycl. Compd.* **2017**, *53*, 1. [CrossRef]
2. Almeida Paz, F.A.; Klinowski, J.; Vilela, S.M.F.; Tomé, J.P.C.; Cavaleiro, J.A.S.; Rocha, J. Ligand design for functional metal–organic frameworks. *Chem. Soc. Rev.* **2012**, *41*, 1088–1110. [CrossRef]
3. Vasconcelos, S.N.S.; Reis, J.S.; de Oliveira, I.M.; Balfour, M.N.; Stefani, H.A. Synthesis of symmetrical biaryl compounds by homocoupling reaction. *Tetrahedron* **2019**, *75*, 1865–1959. [CrossRef]
4. Hassan, J.; Sévignon, M.; Gozzi, C.; Schulz, E.; Lemaire, M. Aryl–Aryl Bond Formation One Century after the Discovery of the Ullmann Reaction. *Chem. Rev.* **2002**, *102*, 1359–1470. [CrossRef]
5. Mondal, S. Recent advancement of Ullmann-type coupling reactions in the formation of C–C bond. *ChemTexts* **2016**, *2*, 17. [CrossRef]
6. Yin, G.; Wang, Z.; Chen, A.; Gao, M.; Wu, A.; Pan, Y. A New Facile Approach to the Synthesis of 3-Methylthio-Substituted Furans, Pyrroles, Thiophenes, and Related Derivatives. *J. Org. Chem.* **2008**, *73*, 3377–3383. [CrossRef]
7. Aponick, A.; Li, C.-Y.; Malinge, J.; Marques, E.F. An Extremely Facile Synthesis of Furans, Pyrroles, and Thiophenes by the Dehydrative Cyclization of Propargyl Alcohols. *Org. Lett.* **2009**, *11*, 4624–4627. [CrossRef]
8. Fustero, S.; Simón-Fuentes, A.; Sanz-Cervera, J.F. Recent Advances in the Synthesis of Pyrazoles. A Review. *Org. Prep. Proced. Int.* **2009**, *41*, 253–290. [CrossRef]
9. Trofimenko, S. 1,1,2,2-Ethanetetracarboxaldehyde and Its Reactions. *J. Org. Chem.* **1964**, *29*, 3046–3049. [CrossRef]
10. Kornfeld, E.C.; Jones, R.G. The Synthesis Oof Furan, Thiophene, and Pyrrole-3,4-Dicarboxylic Esters. *J. Org. Chem.* **1954**, *19*, 1671–1680. [CrossRef]
11. Trofimenko, S. Coordination chemistry of pyrazole-derived ligands. *Chem. Rev.* **1972**, *72*, 497–509. [CrossRef]
12. Weis, C.D. Polycyanofurans. *J. Org. Chem.* **1962**, *27*, 3514–3520. [CrossRef]
13. Boldog, I.; Sieler, J.; Chernega, A.N.; Domasevitch, K.V. 4,4′-Bipyrazolyl: New bitopic connector for construction of coordination networks. *Inorg. Chim. Acta* **2002**, *338*, 69–77. [CrossRef]
14. Arnold, Z. Synthetic reactions of dimethylformamide. XV. Synthesis of symmetrical tetraformylethane. *Collect. Czechoslov. Chem. Commun.* **1962**, *27*, 2993–2995. [CrossRef]
15. Abdel-Wahab, B.F.; Dawood, K.M. Synthesis and applications of bipyrazole systems. *ARKIVOC* **2012**. [CrossRef]
16. Jover, J.; Spuhler, P.; Zhao, L.; McArdle, C.; Maseras, F. Toward a mechanistic understanding of oxidative homocoupling: The Glaser–Hay reaction. *Catal. Sci. Technol.* **2014**, *4*, 4200–4209. [CrossRef]
17. Do, H.-Q.; Daugulis, O. An Aromatic Glaser–Hay Reaction. *J. Am. Chem. Soc.* **2009**, *131*, 17052–17053. [CrossRef]
18. Li, Y.; Jin, J.; Qian, W.; Bao, W. An efficient and convenient Cu(OAc)2/air mediated oxidative coupling of azoles via C–H activation. *Org. Biomol. Chem.* **2010**, *8*, 326–330. [CrossRef]
19. Biffis, A.; Centomo, P.; Del Zotto, A.; Zecca, M. Pd Metal Catalysts for Cross-Couplings and Related Reactions in the 21st Century: A Critical Review. *Chem. Rev.* **2018**, *118*, 2249–2295. [CrossRef]
20. Miyaura, N.; Suzuki, A. Palladium-Catalyzed Cross-Coupling Reactions of Organoboron Compounds. *Chem. Rev.* **1995**, *95*, 2457–2483. [CrossRef]

21. Adamo, C.; Amatore, C.; Ciofini, I.; Jutand, A.; Lakmini, H. Mechanism of the Palladium-Catalyzed Homocoupling of Arylboronic Acids: Key Involvement of a Palladium Peroxo Complex. *J. Am. Chem. Soc.* **2006**, *128*, 6829–6836. [CrossRef] [PubMed]

22. Salanouve, E.; Retailleau, P.; Janin, Y.L. Few unexpected results from a Suzuki–Miyaura reaction. *Tetrahedron* **2012**, *68*, 2135–2140. [CrossRef]

23. Batchu, H.; Bhattacharyya, S.; Kant, R.; Batra, S. Palladium-Catalyzed Chelation-Assisted Regioselective Oxidative Dehydrogenative Homocoupling/Ortho-Hydroxylation in N-Phenylpyrazoles. *J. Org. Chem.* **2015**, *80*, 7360–7374. [CrossRef] [PubMed]

24. Afanas'ev, O.; Tsyplenkova, O.; Seliverstov, M.; Sosonyuk, S.; Proskurnina, M.; Zefirov, N. Homocoupling of bromotriazole derivatives on metal complex catalysts. *Russ. Chem. Bull.* **2015**, *64*, 1470–1472. [CrossRef]

25. Jansa, J.; Schmidt, R.; Mamuye, A.D.; Castoldi, L.; Roller, A.; Pace, V.; Holzer, W. Synthesis of tetrasubstituted pyrazoles containing pyridinyl substituents. *Beilstein J. Org. Chem.* **2017**, *13*, 895–902. [CrossRef]

26. Zhu, J.; Chen, Y.; Lin, F.; Wang, B.; Huang, Q.; Liu, L. Highly Regioselective Arylation of 1,2,3-Triazole N-Oxides with Sodium Arenesulfinates via Palladium-Catalyzed Desulfitative Cross-Coupling Reaction. *Synlett* **2015**, *26*, 1124–1130. [CrossRef]

27. Peng, X.; Huang, P.; Jiang, L.; Zhu, J.; Liu, L. Palladium-catalyzed highly regioselective oxidative homocoupling of 1,2,3-triazole N-oxides. *Tetrahedron Lett.* **2016**, *57*, 5223–5226. [CrossRef]

28. Taylor, M.K.; Juhl, M.; Hadaf, G.B.; Hwang, D.; Velasquez, E.; Oktawiec, J.; Lefton, J.B.; Runčevski, T.; Long, J.R.; Lee, J.-W. Palladium-catalyzed oxidative homocoupling of pyrazole boronic esters to access versatile bipyrazoles and the flexible metal–organic framework Co(4,4′-bipyrazolate). *Chem. Commun.* **2020**, *56*, 1195–1198. [CrossRef]

29. Ackermann, L.; Novák, P.; Vicente, R.; Pirovano, V.; Potukuchi, H.K. Ruthenium-Catalyzed C-H Bond Functionalizations of 1,2,3-Triazol-4-yl-Substituted Arenes: Dehydrogenative Couplings Versus Direct Arylations. *Synthesis* **2010**, *2010*, 2245–2253. [CrossRef]

30. Tasker, S.Z.; Standley, E.A.; Jamison, T.F. Recent advances in homogeneous nickel catalysis. *Nature* **2014**, *509*, 299–309. [CrossRef]

31. Hazari, N.; Melvin, P.R.; Beromi, M.M. Well-defined nickel and palladium precatalysts for cross-coupling. *Nat. Rev. Chem.* **2017**, *1*, 0025. [CrossRef] [PubMed]

32. Fanni, S.; Di Pietro, C.; Serroni, S.; Campagna, S.; Vos, J.G. Ni(0) catalysed homo-coupling reactions: A novel route towards the synthesis of multinuclear ruthenium polypyridine complexes featuring made-to-order properties. *Inorg. Chem. Commun.* **2000**, *3*, 42–44. [CrossRef]

33. Leahy, D.K.; Evans, P.A. Front Matter. In *Modern Rhodium-Catalyzed Organic Reactions*; Evans, P.A., Ed.; Wiley-VCH: Weinheim, Germany, 2005. [CrossRef]

34. Li, S.-S.; Qin, L.; Dong, L. Rhodium-catalyzed C–C coupling reactions via double C–H activation. *Org. Biomol. Chem.* **2016**, *14*, 4554–4570. [CrossRef] [PubMed]

35. Fagnou, K.; Lautens, M. Rhodium-Catalyzed Carbon−Carbon Bond Forming Reactions of Organometallic Compounds. *Chem. Rev.* **2003**, *103*, 169–196. [CrossRef] [PubMed]

36. Albano, G.; Aronica, L.A. From Alkynes to Heterocycles through Metal-Promoted Silylformylation and Silylcarbocyclization Reactions. *Catalysts* **2020**, *10*, 1012. [CrossRef]

37. Kaur, N. Recent developments in the synthesis of nitrogen containing five-membered polyheterocycles using rhodium catalysts. *Synth. Commun.* **2018**, *48*, 2457–2474. [CrossRef]

38. Song, G.; Wang, F.; Li, X. C–C, C–O and C–N bond formation via rhodium(iii)-catalyzed oxidative C–H activation. *Chem. Soc. Rev.* **2012**, *41*, 3651–3678. [CrossRef]

39. Chen, W.-W.; Xu, M.-H. Recent advances in rhodium-catalyzed asymmetric synthesis of heterocycles. *Org. Biomol. Chem.* **2017**, *15*, 1029–1050. [CrossRef]

40. Yue, Y.; Yamamoto, H.; Yamane, M. Rhodium-Catalyzed Homocoupling of (1-Acyloxyvinyl)silanes: Synthesis of 1,3-Diene-2,3-diyl Diesters and Their Derivatives. *Synlett* **2009**, *2009*, 2831–2835. [CrossRef]

41. Luque, R.; Baruwati, B.; Varma, R.S. Magnetically separable nanoferrite-anchored glutathione: Aqueous homocoupling of arylboronic acids under microwave irradiation. *Green Chem.* **2010**, *12*, 1540–1543. [CrossRef]

42. Toshifumi, D.; Yasuyuki, K. Metal-Free Oxidative Biaryl Coupling by Hypervalent Iodine Reagents. *Curr. Org. Chem.* **2016**, *20*, 580–615. [CrossRef]

43. Schulz, M.; Meske, M. Radikalreaktionen an N-Heterocyclen. XI [1] Reaktionen von 3-Methyl-pyrazolin-5-onen mit Phenoxyl-Radikalen. *J. Für Prakt. Chem./Chem.-Ztg.* **1993**, *335*, 607–615. [CrossRef]

44.	Veibel, S. Pyrazole Studies. Xiii. Oxidation by Air of 4-Substituted Pyrazole-5-ones and Stereochemistry of the Oxidation Products. *Acta Chem. Scand.* **1972**, *26*, 3685–3990. [CrossRef]

45.	Sheng, X.; Zhang, J.; Yang, H.; Jiang, G. Tunable Aerobic Oxidative Hydroxylation/Dehydrogenative Homocoupling of Pyrazol-5-ones under Transition-Metal-Free Conditions. *Org. Lett.* **2017**, *19*, 2618–2621. [CrossRef]

46.	Eller, G.A.; Vilkauskaitė, G.; Šačkus, A.; Martynaitis, V.; Mamuye, A.D.; Pace, V.; Holzer, W. An unusual thionyl chloride-promoted C−C bond formation to obtain 4,4′-bipyrazolones. *Beilstein J. Org. Chem.* **2018**, *14*, 1287–1292. [CrossRef]

47.	Li, M.; Zhao, G.; Wen, L.; Wang, X.; Zou, X.; Yang, H. A Coupling Reaction of 4-Amino-5-mercapto-3-substituted-1,2,4-triazoles to Generate Symmetrically Substituted Hydrazines. *Mon. Für Chem./Chem. Mon.* **2005**, *136*, 2045–2049. [CrossRef]

48.	Li, S.H.; Pang, S.P.; Li, X.T.; Yu, Y.Z.; Zhao, X.Q. Synthesis of new tetrazene(N–NN–N)-linked bi(1,2,4-triazole). *Chin. Chem. Lett.* **2007**, *18*, 1176–1178. [CrossRef]

49.	Eğe, S.N.; Tien, C.J.; Dlesk, A.; Potter, B.E.; Eagleson, B.K. Photochemical oxidation of pyrazolidinones. *Chem. Soc. Chem. Commun.* **1972**, 682–683. [CrossRef]

50.	Xiao-Liu, L.I.; Song, Z.-Y.; Meng, J.-B. A novel photochemical reaction of 4-bromo-3-methyl-1-phenyl-4,5-dihydro-pyrazol-5-one. *Chin. J. Chem.* **2004**, *22*, 1215–1218. [CrossRef]

51.	Yuan, X.; Yao, J.-F.; Tang, Z.-Y. Decarboxylative Fluorination of Electron-Rich Heteroaromatic Carboxylic Acids with Selectfluor. *Org. Lett.* **2017**, *19*, 1410–1413. [CrossRef]

52.	Khripun, A.V.; Selivanov, S.I.; Kukushkin, V.Y.; Haukka, M. Hydrogen bonding patterns in pyrazole Pt(II- and IV) chloride complexes. *Inorg. Chim. Acta* **2006**, *359*, 320–326. [CrossRef]

53.	Dang, D.; Li, H.; Zheng, G.; Bai, Y. Synthesis, Crystal Structure and Luminescent Properties of One Silver Complex with 3,5-Diphenylpyrazole. *J. Chem. Crystallogr.* **2011**, *41*, 1612–1615. [CrossRef]

54.	Brandi-Blanco, P.; Miguel, P.J.S.; Lippert, B. Coordination of two different metal ions as reason for N-chirality in μ-amide complexes. *Dalton Trans.* **2011**, *40*, 10316–10318. [CrossRef] [PubMed]

55.	Omary, M.A.; Elbjeirami, O.; Gamage, C.S.P.; Sherman, K.M.; Dias, H.V.R. Sensitization of Naphthalene Monomer Phosphorescence in a Sandwich Adduct with an Electron-Poor Trinuclear Silver(I) Pyrazolate Complex. *Inorg. Chem.* **2009**, *48*, 1784–1786. [CrossRef] [PubMed]

56.	Pettinari, C.; Tăbăcaru, A.; Boldog, I.; Domasevitch, K.V.; Galli, S.; Masciocchi, N. Novel Coordination Frameworks Incorporating the 4,4′-Bipyrazolyl Ditopic Ligand. *Inorg. Chem.* **2012**, *51*, 5235–5245. [CrossRef] [PubMed]

57.	Cui, W.-G.; Hu, T.-L.; Bu, X.-H. Metal–Organic Framework Materials for the Separation and Purification of Light Hydrocarbons. *Adv. Mater.* **2020**, *32*, 1806445. [CrossRef]

58.	Kreno, L.E.; Leong, K.; Farha, O.K.; Allendorf, M.; Van Duyne, R.P.; Hupp, J.T. Metal–Organic Framework Materials as Chemical Sensors. *Chem. Rev.* **2012**, *112*, 1105–1125. [CrossRef]

59.	Xie, L.S.; Skorupskii, G.; Dincă, M. Electrically Conductive Metal–Organic Frameworks. *Chem. Rev.* **2020**, *120*, 8536–8580. [CrossRef]

60.	Horcajada, P.; Gref, R.; Baati, T.; Allan, P.K.; Maurin, G.; Couvreur, P.; Férey, G.; Morris, R.E.; Serre, C. Metal–Organic Frameworks in Biomedicine. *Chem. Rev.* **2012**, *112*, 1232–1268. [CrossRef]

61.	Wang, H.; Zhu, Q.-L.; Zou, R.; Xu, Q. Metal-Organic Frameworks for Energy Applications. *Chem* **2017**, *2*, 52–80. [CrossRef]

62.	Pettinari, C.; Tăbăcaru, A.; Galli, S. Coordination polymers and metal–organic frameworks based on poly(pyrazole)-containing ligands. *Coord. Chem. Rev.* **2016**, *307*, 1–31. [CrossRef]

63.	Spirkl, S.; Grzywa, M.; Reschke, S.; Fischer, J.K.H.; Sippel, P.; Demeshko, S.; Krug von Nidda, H.-A.; Volkmer, D. Single-Crystal to Single-Crystal Transformation of a Nonporous Fe(II) Metal–Organic Framework into a Porous Metal–Organic Framework via a Solid-State Reaction. *Inorg. Chem.* **2017**, *56*, 12337–12347. [CrossRef] [PubMed]

64.	Spirkl, S.; Grzywa, M.; Volkmer, D. Synthesis and characterization of a flexible metal organic framework generated from MnIII and the 4,4′-bipyrazolate-ligand. *Dalton Trans.* **2018**, *47*, 8779–8786. [CrossRef] [PubMed]

65.	Xu, Z.; Han, L.L.; Zhuang, G.L.; Bai, J.; Sun, D. In Situ Construction of Three Anion-Dependent Cu(I) Coordination Networks as Promising Heterogeneous Catalysts for Azide–Alkyne "Click" Reactions. *Inorg. Chem.* **2015**, *54*, 4737–4743. [CrossRef]

66. Lin, R.-B.; Li, T.-Y.; Zhou, H.-L.; He, C.-T.; Zhang, J.-P.; Chen, X.-M. Tuning fluorocarbon adsorption in new isoreticular porous coordination frameworks for heat transformation applications. *Chem. Sci.* **2015**, *6*, 2516–2521. [CrossRef]

67. Li, L.; Yi, J.-D.; Fang, Z.-B.; Wang, X.-S.; Liu, N.; Chen, Y.-N.; Liu, T.-F.; Cao, R. Creating Giant Secondary Building Layers via Alkali-Etching Exfoliation for Precise Synthesis of Metal–Organic Frameworks. *Chem. Mater.* **2019**, *31*, 7584–7589. [CrossRef]

68. Tomar, K.; Rajak, R.; Sanda, S.; Konar, S. Synthesis and Characterization of Polyhedral-Based Metal–Organic Frameworks Using a Flexible Bipyrazole Ligand: Topological Analysis and Sorption Property Studies. *Cryst. Growth Des.* **2015**, *15*, 2732–2741. [CrossRef]

69. Kumar, S.; Arora, A.; Kaushal, J.; Oswal, P.; Kumar, A.; Tomar, K. Room temperature synthesis of an Fe(ii)-based porous MOF with multiple open metal sites for high gas adsorption properties. *New J. Chem.* **2019**, *43*, 4338–4341. [CrossRef]

70. Lin, X.-Y.; Zheng, Q.-Q.; Liu, X.-Z.; Jiang, X.-Y.; Lin, C. Synthesis and thermal stability study of a cobalt-organic framework with tetrahedral cages. *Inorg. Chem. Commun.* **2016**, *67*, 51–54. [CrossRef]

71. Ling, X.-Y.; Wang, J.; Gong, C.; Lu, L.; Singh, A.K.; Kumar, A.; Sakiyama, H.; Yang, Q.; Liu, J. Modular construction, magnetism and photocatalytic properties of two new metal-organic frameworks based on a semi-rigid tetracarboxylate ligand. *J. Solid State Chem.* **2019**, *277*, 673–679. [CrossRef]

72. Huang, M.-J.; Deng, X.; Xian, W.-R.; Liao, W.-M.; He, J. Anion-directed structures and luminescences of two Cu(I) coordination polymers based on bipyrazole. *Inorg. Chem. Commun.* **2019**, *101*, 121–124. [CrossRef]

73. Han, L.-L.; Hu, T.-P.; Mei, K.; Guo, Z.-M.; Yin, C.; Wang, Y.-X.; Zheng, J.; Wang, X.-P.; Sun, D. Solvent-controlled three families of Zn(ii) coordination compounds: Synthesis, crystal structure, solvent-induced structural transformation, supramolecular isomerism and photoluminescence. *Dalton Trans.* **2015**, *44*, 6052–6061. [CrossRef] [PubMed]

74. Han, L.-L.; Wang, Y.-X.; Guo, Z.-M.; Yin, C.; Hu, T.-P.; Wang, X.-P.; Sun, D. Synthesis, crystal structure, thermal stability, and photoluminescence of a 3-D silver(I) network with twofold interpenetrated dia-f topology. *J. Coord. Chem.* **2015**, *68*, 1754–1764. [CrossRef]

75. Huang, X.-H.; Xiao, Z.-P.; Wang, F.-L.; Li, T.; Wen, M.; Wu, S.-T. Syntheses and characterizations of two silver(I) coordination polymers constructed from bipyrazole and dicarboxylate ligands. *J. Coord. Chem.* **2015**, *68*, 1743–1753. [CrossRef]

76. Young, R.J.; Begg, S.L.; Coghlan, C.J.; McDevitt, C.A.; Sumby, C.J. Exploring the Use of Structure and Polymer Incorporation to Tune Silver Ion Release and Antibacterial Activity of Silver Coordination Polymers. *Eur. J. Inorg. Chem.* **2018**, *2018*, 3512–3518. [CrossRef]

77. Singh, U.P.; Singh, N.; Chandra, S. Construction and structural diversity of Cd-MOFs with pyrazole based flexible ligands and positional isomer of naphthalenedisulfonate. *Inorg. Chem. Commun.* **2015**, *61*, 35–40. [CrossRef]

78. Tomar, K.; Gupta, A.K.; Gupta, M. Change in synthetic strategy for MOF fabrication: From 2D non-porous to 3D porous architecture and its sorption and emission property studies. *New J. Chem.* **2016**, *40*, 1953–1956. [CrossRef]

79. Mosca, N.; Vismara, R.; Fernandes, J.A.; Casassa, S.; Domasevitch, K.V.; Bailón-García, E.; Maldonado-Hódar, F.J.; Pettinari, C.; Galli, S. CH3-Tagged Bis(pyrazolato)-Based Coordination Polymers and Metal–Organic Frameworks: An Experimental and Theoretical Insight. *Cryst. Growth Des.* **2017**, *17*, 3854–3867. [CrossRef]

80. Mosca, N.; Vismara, R.; Fernandes, J.A.; Pettinari, C.; Galli, S. The Hg(3,3′-dimethyl-1H,1H′-4,4′-bipyrazolate) coordination polymer: Synthesis, crystal structure and thermal behavior. *Inorg. Chim. Acta* **2018**, *470*, 423–427. [CrossRef]

81. Vismara, R.; Tuci, G.; Tombesi, A.; Domasevitch, K.V.; Di Nicola, C.; Giambastiani, G.; Chierotti, M.R.; Bordignon, S.; Gobetto, R.; Pettinari, C.; et al. Tuning Carbon Dioxide Adsorption Affinity of Zinc(II) MOFs by Mixing Bis(pyrazolate) Ligands with N-Containing Tags. *ACS Appl. Mater. Interfaces* **2019**, *11*, 26956–26969. [CrossRef]

82. Nowacka, A.; Vismara, R.; Mercuri, G.; Moroni, M.; Palomino, M.; Domasevitch, K.V.; Di Nicola, C.; Pettinari, C.; Giambastiani, G.; Llabrés i Xamena, F.X.; et al. Cobalt(II) Bipyrazolate Metal–Organic Frameworks as Heterogeneous Catalysts in Cumene Aerobic Oxidation: A Tag-Dependent Selectivity. *Inorg. Chem.* **2020**, *59*, 8161–8172. [CrossRef] [PubMed]

Publisher's Note: MDPI stays neutral with regard to jurisdictional claims in published maps and institutional affiliations.